Identification of SRGAP2 as a Potential Oncogene and a Prognostic Biomarker in Hepatocellular Carcinoma Using Bioinformatics Analyses and Biological Experiments

Yan Li
Xi'an Jiaotong University Second Affiliated Hospital
Lu Qiao
Xi'an Jiaotong University Second Affiliated Hospital
Yuru Bai
Xi'an Jiaotong University Second Affiliated Hospital
Cailan Xiao
Xi'an Jiaotong University Second Affiliated Hospital Department of Oncology
Jian Wu
Fourth Military Medical University: Air Force Medical University
Xiaoliang Gao
Fourth Military Medical University: Air Force Medical University
Chenyang Qiao
Fourth Military Medical University: Air Force Medical University
Yongquan Shi
Fourth Military Medical University: Air Force Medical University
Wei Hou
Xi'an Jiaotong University Second Affiliated Hospital
Jinhai Wang
Xi'an Jiaotong University Second Affiliated Hospital
Ning Xie
Xi'an Jiaotong University Second Affiliated Hospital
Na Liu (liuna1@xjtu.edu.cn)
Xi'an Jiaotong University Second Affiliated Hospital https://orcid.org/0000-0003-3246-9674

Primary research

Keywords: SRGAPs, SRGAP2, hepatocellular carcinoma, prognosis, metastasis, high-throughput RNA sequencing

Posted Date: December 1st, 2020

DOI: https://doi.org/10.21203/rs.3.rs-113484/v1

Abstract

Background: Hepatocellular carcinoma (HCC) is one of the common malignancies worldwide. Slit-Robo GTPase-activating proteins (SRGAPs) have been shown to regulate the occurrence and development of various tumors. However, their specific role in HCC remains elusive.

Methods: The expression pattern, genetic alteration and prognostic value of SRGAPs in HCC are analyzed by bioinformatics tools. The biological functions of SRGAP2 in HCC cells are demonstrated by in vitro experiments. The high-throughput RNA sequencing is conducted to explore the underlying molecular mechanisms of SRGAP2 in HCC cells.

Results: The expression levels of SRGAP1 and SRGAP2 are significantly elevated in HCC tissues compared to the normal both in Oncomine and TCGA datasets, and SRGAP2 are dramatically upregulated both in mRNA and protein levels. Moreover, higher SRGAP2 is significantly related to the clinical stages of HCC. Meanwhile, SRGAP2 might be an independent prognostic indicator, as it correlates negatively with the clinical outcomes of HCC patients. Further SRGAP2-silencing experiments imply that SRGAP2 might remarkably promote the migration and invasion of HCC cells in EMT-independent manners. Based on the high-throughput RNA sequencing of SRGAP2-knockdown HCC cells, enrichment and network analyses demonstrate that SRGAP2 is closely associated with cellular metabolic signaling.

Conclusions: Our study firstly illustrates the crucial role of SRGAP2 in the metastasis of HCC and explores its underlying molecular mechanisms. We identify SRGAP2 as a promising prognostic biomarker and a novel therapeutic target for HCC patients.

1. Background

Liver cancer is the sixth most commonly diagnosed cancer and the fourth leading cause of cancer deaths around the world [1]. Hepatocellular carcinoma (HCC), as the major form of primary liver cancer, accounts for 85–90% of liver cancer cases worldwide [2]. Many risk factors are associated with HCC, which comprise of not only chronic viruses' infections, alcoholic cirrhosis, diabetes and obesity, but also multiple genes involved in tumorigenesis and metastasis [3, 4]. Despite that the diagnosis, multimodal treatments and perioperative management have been improved over the past years, HCC is commonly diagnosed at the advanced stages due to the scarcity of specific markers for early diagnosis. Thus, it is urgent to identify effectively novel diagnostic and therapeutic strategies for HCC patients.

Slit-Roundabout (Robo) GTPase-activating proteins (SRGAPs), which are firstly identified as the downstream effectors of Slit–Robo signaling, contain four members: SRGAP1, SRGAP2, SRGAP3 and ARHGAP4. Generally, SRGAPs consist of three high conserved domains: N-terminal F-Bin-Amphiphysin-Rvs (BAR) domain, central GTPase-activating proteins (GAPs) domain and C-terminal SH3 domain [5]. F-BAR domain mainly exists in membrane-associated proteins and regulates the interaction between cells and phospholipid membranes with a series of curvatures [6]. Through central GAP domains, SRGAPs could regulate the activity of Rho GTPase family members and then modulate cytoskeletal dynamics during varieties of biological processes [7]. SH3 domain mainly interacts with the intercellular domain of the Robo family receptors to regulate a series of biological activities [5, 8]. Besides, SH3 domain of SRGAPs plays a critical role in their interactions with proteins involved in modulation of actin structure, cell migration and cell adhesion, such as WASF1 [9] and RAPH1 [10].

To date, the focus of studies has been mainly on the key roles of SRGAPs in neuronal development and brain evolution. While, growing evidences have indicated that aberrant expression of SRGAPs participates in regulating the cancer progression. For example, Feng find that downregulation of SRGAP1 is related to tumor progression and poor clinical outcomes in colorectal cancer [11]. Whereas, it is overexpressed in gastric cancer and could function as an oncogene via activating Wnt/β-catenin signaling [12]. SRGAP2 might act as a tumor suppressor in osteosarcoma [13]. In addition, ARHGAP4 overexpression could promote pancreatic tumorigenesis by regulating several signal pathways, such as HDAC2/β-catenin [14], mTOR and HIF-1α signaling pathways [15]. However, the specific role of SRGAPs in HCC is still unknown.

In this study, we firstly comprehensively explore the expression patterns, genetic alterations and prognostic values of SRGAPs in HCC. We find that SRGAP2 is upregulated in HCC tissues compared with normal liver tissues both in mRNA and protein levels, and associated with the poor prognosis in HCC. Further in vitro experiments demonstrate that SRGAP2 silencing obviously inhibits the migration and invasion capacities of HCC cells. Additionally, functional enrichment analyses based on RNA-sequencing data reveal that

SRGAP2 is involved in cellular metabolic signaling. Our study links the biological functions with the prognostic value of SRGAP2 in HCC, which will facilitate the early diagnosis and molecule-targeted therapy for HCC patients.

2. Materials And Methods

2.1. Oncomine database analysis

Oncomine (http://www.oncomine.org) was utilized to analyze the mRNA expression patterns of SRGAPs in HCC and normal tissues. We plotted the gene expressions data with P value < 0.05 and fold change ≥ 1.5.

2.2. TCGA database analysis

TCGA (https://cancergenome.nih.gov) was utilized to analyze the mRNA expression differences of SRGAPs in HCC and normal tissues, and the prognostic values of SRGAPs in HCC patients. The clinical information about HCC patients from TCGA-LIHC contains 371 cases with complete clinicopathological data and follow-up survey.

2.3. GEPIA database analysis

Gene Expression Profiling Interactive Analysis (GEPIA) (http://gepia.cancer-pku.cn/index.html)[16] is a a comprehensive website resource to visualize the RNA-seq data from TCGA database. In this study, we accessed the correlation between differential expression of SRGAPs and pathological stages using GEPIA. P < 0.05 was considered statistically significant.

2.4. Human Protein Atlas (HPA) Data Analysis

Human Protein Atlas (HPA) is a user-friendly online tool that contains immunohistochemistry-based protein expression profiles for the top 20 most common cancer types. The protein expression levels of SRGAPs in normal liver and HCC tissues were assessed by HPA. As for the fraction of stained cells, staining quantity was quantified into four levels: none, < 25%, 25–75% and > 75%. Protein expression levels were decided by both staining intensity and quantity.

2.5. cBioPortal database analysis

The cBio Cancer Genomics Portal (cBioPortal) (http://www.cbioportal.org/) is a friendly online tool to visualize TCGA data for more than 5,000 tumor samples from 232 cancer studies [17, 18]. The Liver Hepatocellular Carcinoma (TCGA, Firehose Legacy, n = 360) cohort were analyzed in this study. The search parameters included mutations, mRNA expression z-scores and putative copy-number alterations. In addition, DNA methylation analysis was also conducted by the cBioPortal online instructions.

2.6. MEXPRESS tool analysis

The MEXPRESS tool (https://mexpress.be), a user-friendly tool to visualize and interpret TCGA data, comprises of the information on mRNA expression, DNA methylation, clinical data as well as the relationships among these parameters [19]. In our study, the effects of methylation status on expression of SRGAP1 in HCC were assessed via the MEXPRESS.

2.7. Kaplan-Meier plotter analysis

Kaplan-Meier plotter (http://kmplot.com/analysis/) was utilized to analyze the relationship between SRGAPs' gene expression and overall survival and disease-specific survival in HCC based on the hazard ratios (HR) and P-values [20].

2.8. TIMER analysis

Tumor Immune Estimation Resource (TIMER) is a computational tool to systematically analyze the abundance of immune infiltrates, clinical and genomic features across diverse cancer types (https://cistrome.shinyapps.io/timer/) [21]. In this study, we constructed the multivariate Cox regression models of SRGAPs in HCC by TIMER.

2.9. RNA extraction and RNA-Sequencing (RNA-Seq)

We used TRIzol® Reagent (Invitrogen, USA) to extract total RNA from 2 cell lines, Hep3B-shRNA-SRGAP2 and Hep3B-shRNA-NC. RNA sequencing was accomplished by Novel Bioinformatics (Shanghai, China). The transcripts with poly(A)-containing human RNA were analyzed by high-throughput Life technologies Ion Proton Sequencer. 3 biological replicates were conducted for each sample. The differences of the mean log2(FPKM + 1) values between 2 groups were assessed using Student's t test. P < 0.05 was considered statistically significant.

2.10. Functional enrichment analysis

We employed Metascape online software (http://metascape.org) to construct GO (Gene Ontology) and Reactome enrichment analyses of the differentially expressed genes from RNA-Sequencing. All analyses were conducted with default website parameters [22]. Spearman's correlation coefficient exceeding 0.3 indicated a good correlation between SRGAP2 and its differentially expressed genes.

2.11 Cell lines

The human hepatocellular carcinoma cell lines (Hep3B, HepG2 and SMMC-7721) were obtained from the National Infrastructure of Cell Line Resource (China) in 2019. They were maintained in RPMI-1640 medium supplemented with 10% fetal bovine serum and 1% penicillin-streptomycin solution. All cell lines were cultured at 37 °C in a humidified atmosphere containing 5% CO2. All cell lines have been authenticated by short tandem repeat (STR) analysis and tested as free of mycoplasma contamination recently.

2.12 Lentivirus transfection

All lentiviruses were purchased from Genechem (Shanghai, China). According to the instructions, the lentiviruses and cells were incubated in enhanced infection solution with a final volume of 2 ml/well in 6-well plates. 24 hours later, the solution was replaced with fresh RPMI-1640 or DMEM medium containing 10% FBS. 72 hours later, the cells were treated with puromycin (HepG2 and Hep3B: 2.5 μg/mL, SMMC-7721:2 μg/mL), and then the transfection efficiency was verified by western blot analysis.

2.13 Western blot analysis

The specific protocol was reported in a previous study [23]. The antibodies used were as follows: anti-SRGAP2 (at 1:2000, ab124958, Abcam), anti-E-Cadherin (at 1:1000, #3195S, CST), anti-N-cadherin (at 1:1000, #13116S, CST), anti-beta-catenin (at 1:1000, #8480S, CST), anti-Vimentin (at 1:1000, #5741S, CST), anti-Occuldin (at 1:2000, ab52237, Abcam), anti-Fibronectin (at 1:1000, #26836S, CST), anti-GAPDH (at 1:6000, 10494-1-AP, Proteintech Technology) and the corresponding secondary antibodies (at 1:10000, MYBiotech). ImageJ software was used to analyze and quantify each band.

2.14 Transwell migration and invasion assays

The transwell migration assay is to test the cell migration ability by using a chamber (12 mm diameter with 8 um pores, BD, USA). 1×10^5 HCC cells were resuspended by medium without FBS in the upper chambers, then the chambers were placed into the 24-well plates with 10% FBS medium or 3T3 medium. Cells were incubated for 24 hours (SMMC-7721), 48 hours (Hep3B) and 72 hours (HepG2). After fixed with 4% PFA for 30 minutes, cells were stained with 0.05% crystal violet for 20 minutes. Cells were counted under a microscope at 100 × magnification.

The cell invasion assay is to test the cell invasive ability by using a chamber (12 mm diameter with 8 um pores, BD, USA) with matrigel. 1×10^5 HCC cells were resuspended by medium without FBS in the upper chambers with matrigel (#354248, BD, USA), and then the chambers were placed into the 24-well plates with 10% FBS medium or 3T3 medium. The following procedures were the same with those in the migration assay.

2.15 Statistical analyses

The rank sum test was used to reveal the correlation between SRGAP2 expression and clinicopathologic features. Each experiment was repeated independently at least three times. The differences between the two groups were assessed using Student's t test. $P < 0.05$ was accepted as significant differences. We utilized SPSS software (Version 18.0) and GraphPad Prism software (Version 7.0) to conduct statistical analyses and plot the diagrams.

3. Results

1. The expression patterns of SRGAPs in HCC

Firstly, we aimed to explore the mRNA expression status of SRGAPs in multiple public datasets. We found that SRGAP1 and SRGAP2 were significantly upregulated in HCC tissues compared with normal tissues in Wumbach Liver cohort by Oncomine exploration (fold change > 1.5, P < 0.05) (Fig. 1A and 1B). In TCGA LIHC dataset, SRGAP1, SRGAP2, SRGAP3 and ARHGAP4 were all found to be significantly overexpressed in HCC compared with normal tissues (Fig. 1C). Specially, we found that overexpressed SRGAP1 and SRGAP2 was significantly associated with the pathological stage of HCC patients by GEPIA (Fig. S1). The Next, the Human Protein Atlas was used to explore the protein expression differences of SRGAPs between HCC tissues and liver normal tissues. As shown in Fig. 1D and Table 1, medium protein expressions of SRGAP1 were found both in normal liver tissues and HCC tissues. SRGAP2 was low expressed in normal liver tissue, whereas its medium protein expression was observed in HCC tissue. Additionally, SRGAP3 and ARHGAP4 could not be detected both in normal liver tissue and HCC tissue. Generally, our results showed that SRGAP2 was upregulated in patients with HCC both in mRNA and protein levels.

Table 1
The protein expression status of SRGAPs in HCC patients in HPA.

Gene	Antibody	Tissue	Id	Sex	Age	Staining	Intensity	Quantity	Location
SRGAP1	HPA052416	Tumor	2556	Male	72	High	Strong	> 75%	Cytoplasmic/membranous nuclear
		Normal	3222	Female	63	Medium	Moderate	> 75%	Cytoplasmic/membranous nuclear
SRGAP2	HPA028191	Tumor	983	Female	53	Medium	Moderate	> 75%	Cytoplasmic/membranous nuclear
		Normal	3222	Female	63	Not detected	Negative	None	None
SRGAP3	HPA036959	Tumor	None	None	None	Not detected	Negative	None	None
		Normal	2429	Male	55	Not detected	Negative	None	None
ARHGAP4	HPA001012	Tumor	1287	Female	24	Not detected	Negative	None	None
		Normal	667	Female	27	Not detected	Negative	None	None

2. The genetic alterations of SRGAPs in HCC

To integratedly understand the expression patterns of SRGAPs in HCC, we conducted the genetic analysis of SRGAPs via cBioPortal. As shown in Fig. 2A, we found that SRGAP2 displayed the highest mutation ratio (21% in TCGA) of genetic variation in HCC. The mutation ratios of SRGAP1, SRGAP3 and ARHGAP4 were 6%, 6% and 8%, respectively. Additionally, gene amplification, mutation and deep deletion contributed to the dysregulation of SRGAPs in HCC. Specifically, we found that gene amplification was mainly involved in mRNA upregulation of SRGAP2 in HCC (Fig. 2B). From analysis of the protein structure mutation, we found that SRGAP3 had more mutation sites than others (mutation sites = 8) (Fig. 2C). Moreover, as shown in Fig. 2D, DNA methylation analysis indicated that there was a negative correlation between mRNA expression and DNA methylation of SRGAP1 (R = -0.36, P < 0.05). In a word, our results suggested that copy number amplification and (or) DNA methylation might be mainly involved in the epigenetic regulation of SRGAPs.

3. The prognostic values of SRGAPs in HCC

We further investigated the effects of SRGAPs on the overall survival (OS) and disease-specific survival (DSS) of HCC patients based on the Kaplan-Meier (K-M) plotter database. As shown in Fig. 3A, the OS analysis revealed that higher expression level of SRGAP2 was significantly associated with the shorter survival time (HR = 1.81, P = 0.0025). Whereas, SRGAP1, SRGAP3 and ARHGAP4 had no statistically significant impact on OS of HCC patients (P > 0.05). Additionally, the DSS analysis showed that higher expression levels of SRGAP2 (HR = 1.73, P = 0.026) and SRGAP3 (HR = 0.61, P = 0.04) were obviously related to the worse clinical outcomes for HCC

patients (Fig. 3B). TCGA LIHC cohort was also utilized to further evaluate the correlation between SRGAP2 expression and clinical parameters in HCC. The results illustrated that SRGAP2 overexpression was associated with advanced TNM stage (Table 2). Moreover, multivariate Cox regression model indicated that overexpressed SRGAP2 could significantly dampen the overall survival of HCC patients after adjusting several confounding clinical factors, including age, gender, race, stage and purity (Fig. 3C and Table 3). Thus, SRGAP2 was the most significant prognostic biomarker among SRGAPs for HCC patients.

Table 2
The correlation between SRGAP2 mRNA level and characteristic features of HCC patients in TCGA.

		SRGAP2		χ^2	P value
		low expression	high expression		
Age(y)	≤ 61(median)	100	92	0.884	0.347
	> 61	84	94		
Sex	female	59	62	2.499	0.114
	male	126	186		
Grade	G1	10	11	8.553	0.14
	G2	41	19		
	G3	14	22		
TNM stage	I	95	76	7.81	0.049*
	II	35	51		
	III	38	47		
	IV	4	1		
T	T1	69	28	30.195	0.0001****
	T2	29	35		
	T3	26	55		
	T4	4	9		
* P < 0.05, **** P < 0.0001					

Table 3
Multivariate Cox regression analysis of SRGAP2, age, gender, race, stage and purity in relation to overall survival of HCC patients in TCGA dataset (n = 371).

	coef	HR se(coef)	95%CI_l	95%CI_u	z	p signif
SRGAP2	0.336	0.120–1.399	0.120	1.107	1.768	0.005 **
Age	0.013	0.008–1.013	0.997	1.030	1.574	0.116
Gender male	-0.119	0.226–0.888	0.570	1.384	-0.525	0.600
Race Black	0.731	0.494–2.077	0.788	5.472	1.479	0.139
Race White	-0.064	0.238–0.938	0.588	1.494	-0.271	0.787
Stage 2	0.203	0.267–1.225	0.726	2.068	0.761	0.447
Stage 3	0.882	0.238–2.416	1.516	3.851	3.709	0.000 ***
Stage 4	1.674	0.622–5.335	1.577	18.048	2.693	0.007 **
Purity	0.526	0.452–1.693	0.698	4.105	1.164	0.244
Rsquare = 0.108 (max possible = 9.66e-01)						
Likelihood ratio test p = 5.2e-05						
Wald test p = 2.89e-05						
Score (logrank) test p = 8.76e-06 * P < 0.05, **P <0.01, *** P <0.001						

4. SRGAP2 promoted the invasion and migration of HCC cells in vitro

Metastasis significantly contributes to the poor clinical outcomes of HCC patients after surgical resection[24]. However, its molecular mechanisms remain elusive. Given the significance of SRGAP2 in HCC, we aimed to examine whether it might promote the metastatic ability of HCC cells by in vitro experiments. Hep3B, SMMC-7721 and HepG2 were transfected with shRNAs against SRGAP2 and the downregulation efficacy was confirmed by western blot analyses (Fig. 4A and 4B). The transwell assays, as shown in Fig. 4C and 4D, indicated that SRGAP2 knockdown could markedly inhibit the migration and invasion ability of HCC cells. Growing evidences indicate that EMT acquires an essential role in HCC metastasis[25]. To explore the role of SRGAP2 in regulating EMT, we evaluated the expression levels of EMT markers, such as E-cadherin, N-cadherin, occludin and vimentin, after SRGAP2 silencing in HCC cells. However, there was no statistical difference between LV-shSRGAP2 and LV-shcontrol groups (Fig. 4E-4G). Our results, therefore, confirmed that that downregulation of SRGAP2 impaired the migratory and invasive ability of HCC cells in an EMT-independent fashion.

5. The potential downstream mechanisms of SRGAP2 in HCC

High-throughput RNA-sequencing was conducted to identify the genes that are regulated by SRGAP2 in HCC cells. As shown in Fig. 5A, the six samples were screened for gene differential expression with a 3:3 ratio. 1386 upregulated and 1482 downregulated genes between Hep3B-shARL4C and Hep3B-NC groups (FDR < 0.05) had been screened by RNA-sequencing (Fig. 5B and 5C). Pearson's

correlation coefficient exceeding 0.3 suggested a good correlation between SRGAP2 and its differentially expressed genes in HCC cells. Then, we employed the Metascape enrichment tool to perform functional enrichment analyses.

As shown in Fig. 6A and Table S1, the top 20 GO enrichment items for upregulated and downregulated genes were divided into three functional groups: biological process (BP) (15 items), molecular function (MF) (3 item), and cellular component (CC) (2 items). The differentially expressed genes were mainly enriched in several metabolic biological processes, such as monocarboxylic acid metabolic process (gene ratio = 37/664, Log(p-value) = -10.077), organic hydroxy compound metabolic process (gene ratio = 31/556, Log(p-value) = -8.530), glutamine family amino acid metabolic process (gene ratio = 12/76, Log(p-value) = -8.469), cofactor metabolic process (gene ratio = 18/311, Log(p-value) = -7.711), and antibiotic metabolic process (gene ratio = 15/152, Log(p-value) = -7.541). The MFs for these differentially expressed genes were endopeptidase inhibitor activity (gene ratio = 23/183, Log(p-value) = -8.987), receptor regulator activity (gene ratio = 40/534, Log(p-value) = -8.097) and calcium ion binding (gene ratio = 47/712, Log(p-value) = -7.674). Meanwhile, the CCs for these genes were the extracellular matrix (gene ratio = 53/569, Log(p-value) = -14.257) and endoplasmic reticulum lumen (gene ratio = 30/308, Log(p-value) = -8.777).

Consistently, as shown in Fig. 6B-D, Reactome pathway enrichment analysis also demonstrated that SRGAP2 was highly associated with metabolism-related signal pathways: Carbon metabolism (gene ratio = 5/114, Log(p-value) = -3.940215054) and Metabolism of xenobiotics by cytochrome P450 (gene ratio = 3/76, Log(p-value) = -2.407652205). Meanwhile, a gene–gene interaction network conducted via GeneMANIA tool also indicated that there was a close crosstalk between SRGAP2 and genes involved in cellular metabolism, including shared protein domains, physical interactions co-expression and co-localization (Fig. 7).

4. Discussion

Increasing evidences indicate that SRGAPs might play important roles in cancer progression. However, the exact role of SRGAPs in HCC and the underlying molecular mechanisms remain unclear. The present study aims to systematically explore the expression status, genetic alterations, prognostic values and underlying functions of SRGAPs in HCC through bioinformatics analyses and experimental validation.

The mRNA expression profiles of SRGAPs in HCC are firstly explored by Oncomine and TCGA datasets, which demonstrates that SRGAP1 and SRGAP2 are commonly overexpressed in HCC. SRGAP1, the most famous and studied protein of the SRGAPs, is found to play a dual role in cancer progression. On one hand, SRGAP1 is downregulated in CRC tissues and might act as a positive prognostic indicator for CRC patients [11]. On the other hand, SRGAP1 overexpression promotes gastric tumorigenesis and is associated with the poor survival in gastric cancer [26]. In our study, pan-cancer analysis shows that the mRNA expression of SRGAP1 is heterogeneous in different cancers, which also indicates its two-tier functions in different cancer types. Moreover, its overexpression is related to advanced pathological stages of HCC patients. Genetic alteration analysis of SRGAP1 shows that gene amplification and DNA methylation are both involved in SRGAP1 dysregulation in HCC. Specifically, we discover that DNA methylation status is inversely correlated with the SRGAP1 mRNA expression in HCC. It is widely recognized that DNA methylation is a critical epigenetic process that saliently contributes to cancer evolution and development. A recent study shows that SRGAP1 is overexpressed in human skeletal muscle after acute and chronic resistance exercise due to its DNA hypomethylation at cg07973246 site [27]. Consistently, we find that the cg07973246 methylation status is significantly negatively related to SRGAP1 mRNA expression in HCC (**Table S1**). Taken together, we speculate that DNA methylation status might be involved in the dysregulation and oncogenic functions of SRGAP1 in HCC.

SRGAP2 is primarily reported to participate in regulating cortical neuron function [28, 29]. A recent research shows that SRGAP2 can effectively inhibit metastatic ability of osteosarcoma cells [13]. Nevertheless, its expression status, prognostic value and biological function in HCC is still unknown. In this study, we demonstrate that SRGAP2 is significantly upregulated in HCC tissues compared with normal liver tissues both in transcript and protein levels. Meanwhile, only overexpressed SRGAP2 is associated with shorter OS and DSS, and acts as an independent prognostic biomarker for HCC patients among SRGAPs. Thus, we further assess the effects of SRGAP2 on the metastasis ability of HCC cells by in vitro experiments. Our results suggest a close association between SRGAP2 expression and HCC invasive phenotypes, as indicated by the suppressed migration and invasion abilities of HCC cells after SRGAP2 silencing. However, SRGAP2 knockdown could not alter the expression of epithelial marker (E-cadherin) and mesenchymal markers (N-cadherin and vimentin). Although it is reported that EMT plays a critical role in first step of the metastatic process [30], tumor metastasis also often occurs without stimulating EMT program [31]. A recent study shows that AKT-induced lncRNA VAL could promote metastasis of lung adenocarcinoma in the absence of activating EMT [32]. Therefore, our results indicate that SRGAP2 might exert the promoting effects on metastasis of HCC in an EMT-independent manner.

To uncover the underlying mechanisms of SRGAP2 in HCC metastasis, we further analyze the genes expression alteration in HCC cells after SRGAP2 silencing by high-throughput RNA sequencing. Functional enrichment analysis indicates that SRGAP2 is highly correlated with several metabolic processes. Accumulating evidences show a complicated interaction between cellular metabolism and tumor metastasis. Cellular metabolic rewiring could promote cancer metastasis in various manners, including regulating metabolic demands of cancer cells, regulating gene expression to hijack metastatic signaling pathways and modulating metabolites or cofactors to affect proteins involved in metastasis. On the other side, metastatic signaling could also impact metabolic biological processes by directly affecting metabolic enzymes[33, 34]. In this study, we also observe a close crosstalk between SRGAP2 and the genes involved in cellular metabolism. Taken together, our result demonstrates that SRGAP2 might play a crucial role in HCC metastasis via modulating metabolic processes.

5. Conclusions

To our knowledge, it is for the first time that the expression pattern, genetic alteration and clinical relevance of SRGAPs in HCC have been fully illustrated. Our results identify SRGAP2 as an important prognostic biomarker for HCC patient. SRGAP2 might act as an oncogene in HCC progression by promoting cell metastasis. Our studies offer a comprehensive insight into the specific roles of SRGAPs that benefits the development of novel strategies for early detection and molecule targeted therapy in HCC.

Abbreviations

HCC: Hepatocellular carcinoma; SRGAPs: Slit-Robo GTPase-activating proteins; BAR: Bin-Amphiphysin-Rvs; GAPs: GTPase-activating proteins; HPA: Human Protein Atlas; WB: Western blot; RNA-Seq: RNA-Sequencing; K-M: Kaplan-Meier; OS: Overall survival; DSS: Disease-specific survival; BP: Biological process; MF: Molecular function; CC: Cellular component.

Declarations

Authors' Contributions:

Yan Li performed most of the experimental work as well as data analysis. Lu Qiao contributed equally to this work. Yuru Bai and Cailan Xiao assisted with performing prognosis analysis. Jian Wu, Xiaoliang Gao and Chenyang Qiao assisted with cell experiments. Wei Hou and Yongquan Shi assisted with authoring the manuscript. Jinhai Wang provided funding. Ning Xie coordinated the project and authorized the manuscript. Na Liu provided funding and assisted in authoring the manuscript. All authors reviewed the results and approved the final version of the manuscript.

Acknowledgements:

Not applicable.

Competing interests:

The authors declare that they have no competing interests.

Availability of data and materials:

The datasets generated and/or analyzed during the current study are available from the corresponding author on reasonable request.

Consent for publication:

Not applicable.

Ethics approval and consent to participate:

Not applicable.

Funding:

The study was supported by grants from the National Natural Science Foundation of China (No. 81872397).

References

1. Bray F, Ferlay J, Soerjomataram I, Siegel RL, Torre LA, Jemal A: Global cancer statistics 2018: GLOBOCAN estimates of incidence and mortality worldwide for 36 cancers in 185 countries. CA Cancer J Clin 2018.
2. El-Serag HB, Rudolph KL: Hepatocellular carcinoma: epidemiology and molecular carcinogenesis. Gastroenterology 2007, 132(7):2557-2576.
3. Yang JD, Hainaut P, Gores GJ, Amadou A, Plymoth A, Roberts LR: A global view of hepatocellular carcinoma: trends, risk, prevention and management. Nat Rev Gastroenterol Hepatol 2019, 16(10):589-604.
4. Zhang MH, Shen QH, Qin ZM, Wang QL, Chen X: Systematic tracking of disrupted modules identifies significant genes and pathways in hepatocellular carcinoma. Oncol Lett 2016, 12(5):3285-3295.
5. Lucas B, Hardin J: Mind the (sr)GAP - roles of Slit-Robo GAPs in neurons, brains and beyond. J Cell Sci 2017, 130(23):3965-3974.
6. Liu S, Xiong X, Zhao X, Yang X, Wang H: F-BAR family proteins, emerging regulators for cell membrane dynamic changes-from structure to human diseases. J Hematol Oncol 2015, 8:47.
7. Xu R, Qin N, Xu X, Sun X, Chen X, Zhao J: Inhibitory effect of SLIT2 on granulosa cell proliferation mediated by the CDC42-PAKs-ERK1/2 MAPK pathway in the prehierarchical follicles of the chicken ovary. Sci Rep 2018, 8(1):9168.
8. Soderling SH, Binns KL, Wayman GA, Davee SM, Ong SH, Pawson T, Scott JD: The WRP component of the WAVE-1 complex attenuates Rac-mediated signalling. Nat Cell Biol 2002, 4(12):970-975.
9. Soderling SH, Binns KL, Wayman GA, Davee SM, Ong SH, Pawson T, Scott JD: The WRP component of the WAVE-1 complex attenuates Rac-mediated signalling. Nature Cell Biology 2002, 4(12):970-975.
10. Endris V, Haussmann L, Buss E, Bacon C, Bartsch D, Rappold G: SrGAP3 interacts with lamellipodin at the cell membrane and regulates Rac-dependent cellular protrusions. Journal of Cell Science 2011, 124(23):3941-3955.
11. Feng Y, Feng L, Yu D, Zou J, Huang Z: srGAP1 mediates the migration inhibition effect of Slit2-Robo1 in colorectal cancer. Journal of experimental & clinical cancer research : CR 2016, 35(1):191.
12. Huang T, Zhou Y, Zhang J, Wong CC, Li W, Kwan JSH, Yang R, Chan AKY, Dong Y, Wu F et al: SRGAP1, a crucial target of miR-340 and miR-124, functions as a potential oncogene in gastric tumorigenesis. Oncogene 2018, 37(9):1159-1174.
13. Marko TA, Shamsan GA, Edwards EN, Hazelton PE, Rathe SK, Cornax I, Overn PR, Varshney J, Diessner BJ, Moriarity BS et al: Slit-Robo GTPase-Activating Protein 2 as a metastasis suppressor in osteosarcoma. Sci Rep 2016, 6:39059.
14. Shen Y, Xu L, Ning Z, Liu L, Lin J, Chen H, Meng Z: ARHGAP4 regulates the cell migration and invasion of pancreatic cancer by the HDAC2/β-catenin signaling pathway. Carcinogenesis 2019, 40(11):1405-1414.
15. Shen Y, Chen G, Zhuang L, Xu L, Lin J, Liu L: ARHGAP4 mediates the Warburg effect in pancreatic cancer through the mTOR and HIF-1alpha signaling pathways. Onco Targets Ther 2019, 12:5003-5012.
16. Tang Z, Li C, Kang B, Gao G, Li C, Zhang Z: GEPIA: a web server for cancer and normal gene expression profiling and interactive analyses. Nucleic acids research 2017, 45(W1):W98-w102.
17. Cerami E, Gao J, Dogrusoz U, Gross BE, Sumer SO, Aksoy BA, Jacobsen A, Byrne CJ, Heuer ML, Larsson E et al: The cBio cancer genomics portal: an open platform for exploring multidimensional cancer genomics data. Cancer discovery 2012, 2(5):401-404.
18. Gao J, Aksoy BA, Dogrusoz U, Dresdner G, Gross B, Sumer SO, Sun Y, Jacobsen A, Sinha R, Larsson E et al: Integrative analysis of complex cancer genomics and clinical profiles using the cBioPortal. Science signaling 2013, 6(269):pl1.
19. Jing X, Liang H, Hao C, Hongxia L, Cui X: Analyses of an epigenetic switch involved in the activation of pioneer factor FOXA1 leading to the prognostic value of estrogen receptor and FOXA1 co-expression in breast cancer. Aging 2019, 11(18):7442-7456.
20. Gyorffy B, Lanczky A, Eklund AC, Denkert C, Budczies J, Li Q, Szallasi Z: An online survival analysis tool to rapidly assess the effect of 22,277 genes on breast cancer prognosis using microarray data of 1,809 patients. Breast cancer research and treatment 2010, 123(3):725-731.

21. Li T, Fan J, Wang B, Traugh N, Chen Q, Liu JS, Li B, Liu XS: TIMER: A Web Server for Comprehensive Analysis of Tumor-Infiltrating Immune Cells. Cancer research 2017, 77(21):e108-e110.
22. Zhou Y, Zhou B, Pache L, Chang M, Khodabakhshi AH, Tanaseichuk O, Benner C, Chanda SK: Metascape provides a biologist-oriented resource for the analysis of systems-level datasets. Nature communications 2019, 10(1):1523.
23. Liu N, Bi F, Pan Y, Sun L, Xue Y, Shi Y, Yao X, Zheng Y, Fan D: Reversal of the malignant phenotype of gastric cancer cells by inhibition of RhoA expression and activity. Clin Cancer Res 2004, 10(18 Pt 1):6239-6247.
24. Forner A, Reig M, Bruix J: Hepatocellular carcinoma. Lancet (London, England) 2018, 391(10127):1301-1314.
25. Yan L, Xu F, Dai CL: Relationship between epithelial-to-mesenchymal transition and the inflammatory microenvironment of hepatocellular carcinoma. Journal of experimental & clinical cancer research : CR 2018, 37(1):203.
26. Huang T, Zhou Y, Zhang J, Wong C, Li W, Kwan J, Yang R, Chan A, Dong Y, Wu F et al: SRGAP1, a crucial target of miR-340 and miR-124, functions as a potential oncogene in gastric tumorigenesis. Oncogene 2018, 37(9):1159-1174.
27. Turner D, Seaborne R, Sharples A: Comparative Transcriptome and Methylome Analysis in Human Skeletal Muscle Anabolism, Hypertrophy and Epigenetic Memory. Scientific reports 2019, 9(1):4251.
28. Guerrier S, Coutinho-Budd J, Sassa T, Gresset A, Jordan NV, Chen K, Jin WL, Frost A, Polleux F: The F-BAR domain of srGAP2 induces membrane protrusions required for neuronal migration and morphogenesis. Cell 2009, 138(5):990-1004.
29. Charrier C, Joshi K, Coutinho-Budd J, Kim JE, Lambert N, de Marchena J, Jin WL, Vanderhaeghen P, Ghosh A, Sassa T et al: Inhibition of SRGAP2 function by its human-specific paralogs induces neoteny during spine maturation. Cell 2012, 149(4):923-935.
30. Bakir B, Chiarella AM, Pitarresi JR, Rustgi AK: EMT, MET, Plasticity, and Tumor Metastasis. Trends Cell Biol 2020, 30(10):764-776.
31. Dongre A, Weinberg RA: New insights into the mechanisms of epithelial-mesenchymal transition and implications for cancer. Nature reviews Molecular cell biology 2019, 20(2):69-84.
32. Tian H, Lian R, Li Y, Liu C, Liang S, Li W, Tao T, Wu X, Ye Y, Yang X et al: AKT-induced lncRNA VAL promotes EMT-independent metastasis through diminishing Trim16-dependent Vimentin degradation. Nat Commun 2020, 11(1):5127.
33. Wei Q, Qian Y, Yu J, Wong CC: Metabolic rewiring in the promotion of cancer metastasis: mechanisms and therapeutic implications. Oncogene 2020, 39(39):6139-6156.
34. Schild T, Low V, Blenis J, Gomes AP: Unique Metabolic Adaptations Dictate Distal Organ-Specific Metastatic Colonization. Cancer Cell 2018, 33(3):347-354.

Figures

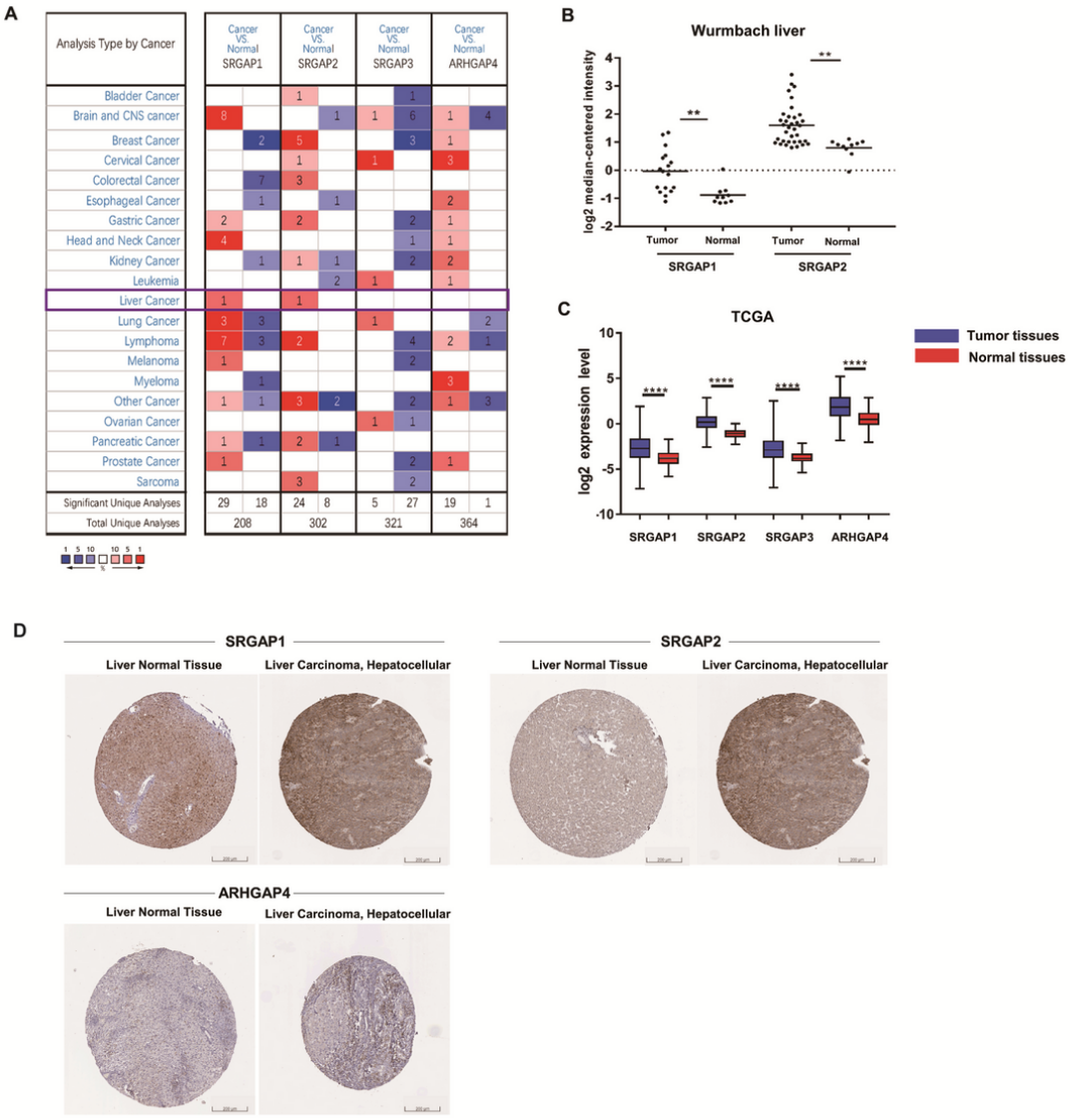

Figure 1

Expression profiles of SRGAPs in HCC. (A) Pan-cancer analysis of the mRNA expression patterns of SRGAPs by Oncomine database. The threshold parameters were set as follows: fold change = 2, P value < 0.05, gene rank = 10%. (B) The expression details of SRGAP1 and SRGAP2 in Wurmbach liver dataset. (C) The expression profiles of SRGAPs in HCC tissues compared with normal tissues (TCGA). * P < 0.05, **P <0.01, *** P <0.001, **** P <0.0001. (D) The protein expression status of SRGAPs in HCC patients in HPA database.

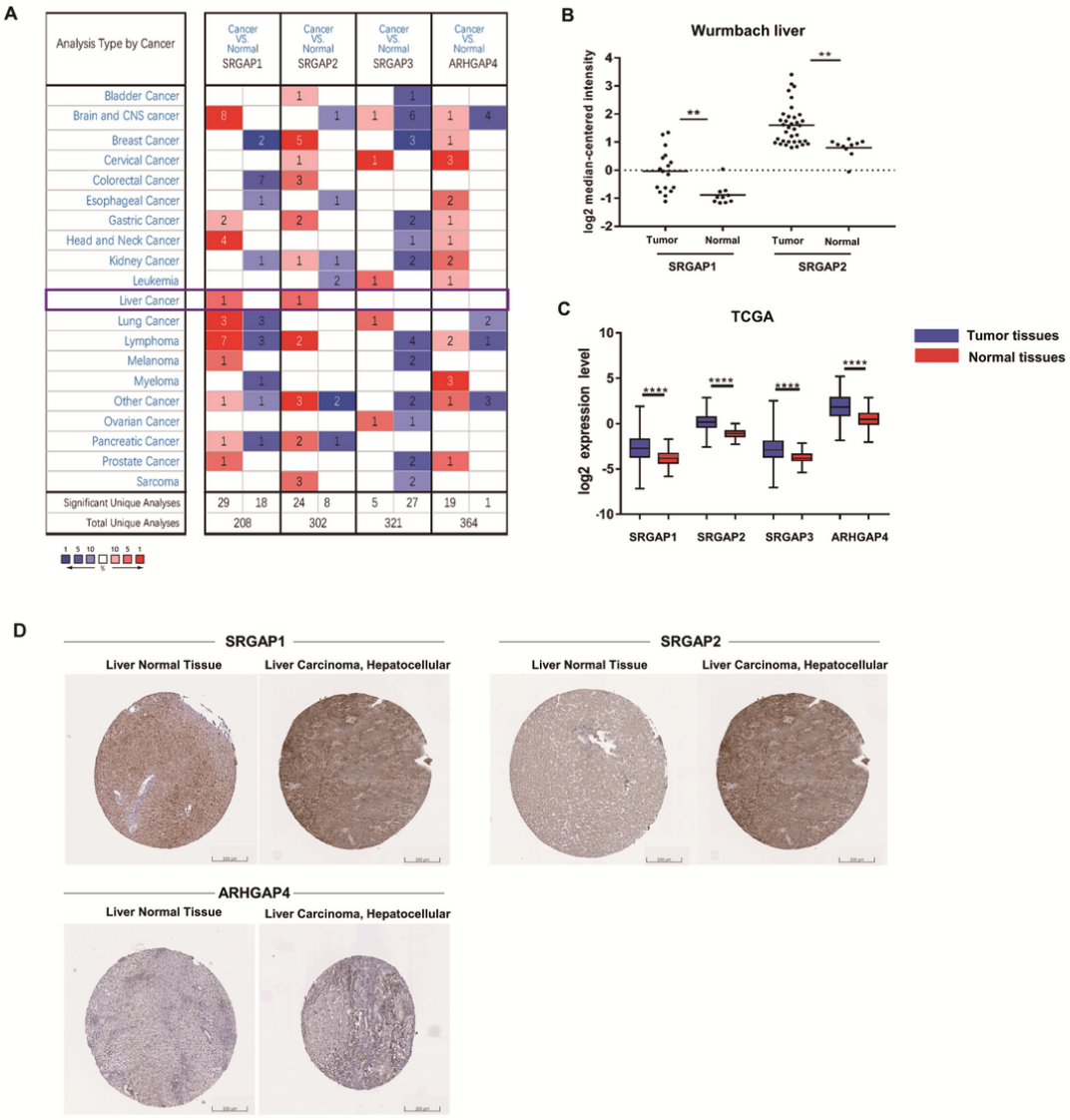

Figure 1

Expression profiles of SRGAPs in HCC. (A) Pan-cancer analysis of the mRNA expression patterns of SRGAPs by Oncomine database. The threshold parameters were set as follows: fold change = 2, P value < 0.05, gene rank = 10%. (B) The expression details of SRGAP1 and SRGAP2 in Wurmbach liver dataset. (C) The expression profiles of SRGAPs in HCC tissues compared with normal tissues (TCGA). * P < 0.05, **P <0.01, *** P <0.001, **** P <0.0001. (D) The protein expression status of SRGAPs in HCC patients in HPA database.

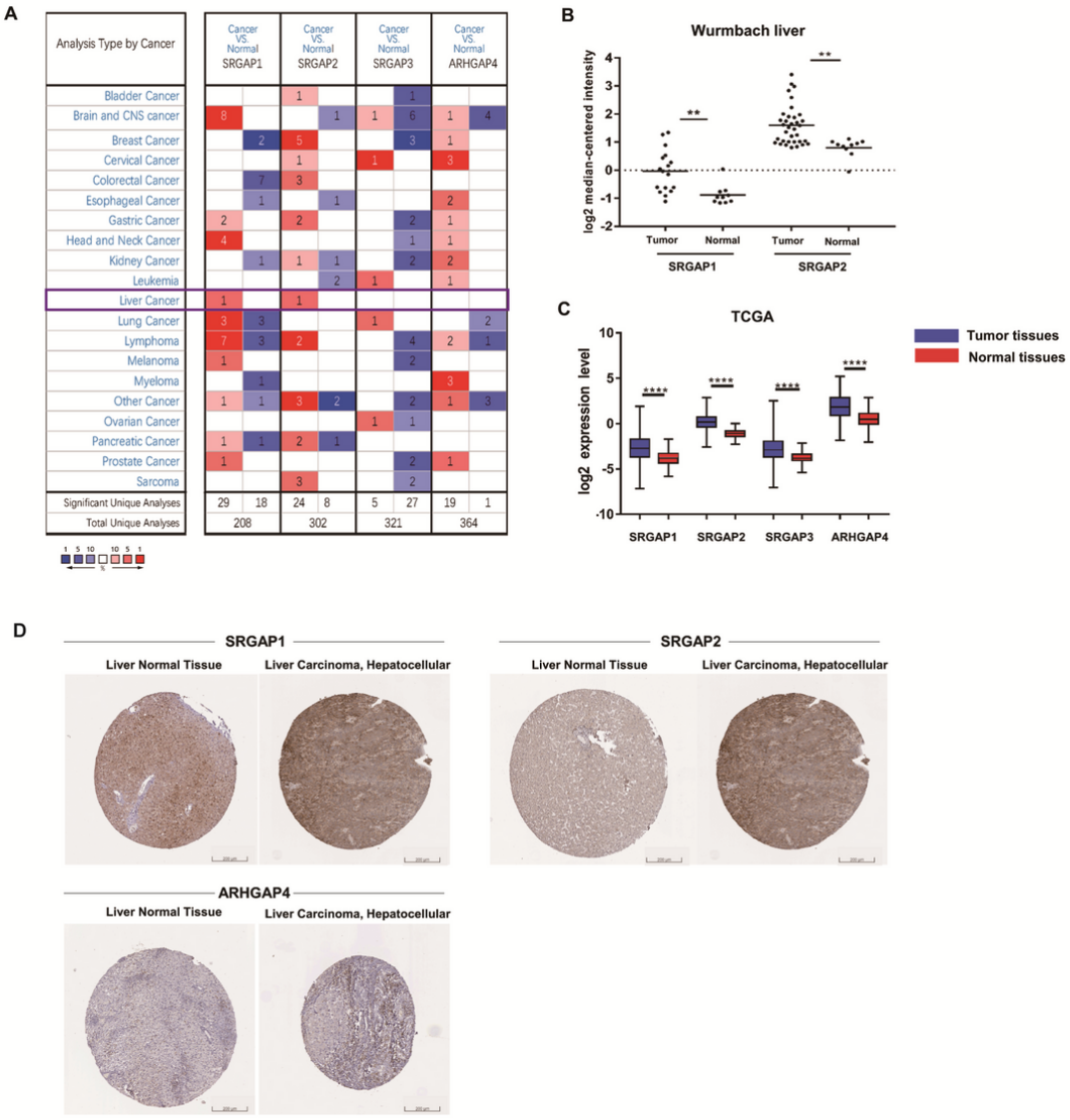

Figure 1

Expression profiles of SRGAPs in HCC. (A) Pan-cancer analysis of the mRNA expression patterns of SRGAPs by Oncomine database. The threshold parameters were set as follows: fold change = 2, P value < 0.05, gene rank = 10%. (B) The expression details of SRGAP1 and SRGAP2 in Wurmbach liver dataset. (C) The expression profiles of SRGAPs in HCC tissues compared with normal tissues (TCGA). * P < 0.05, **P <0.01, *** P <0.001, **** P <0.0001. (D) The protein expression status of SRGAPs in HCC patients in HPA database.

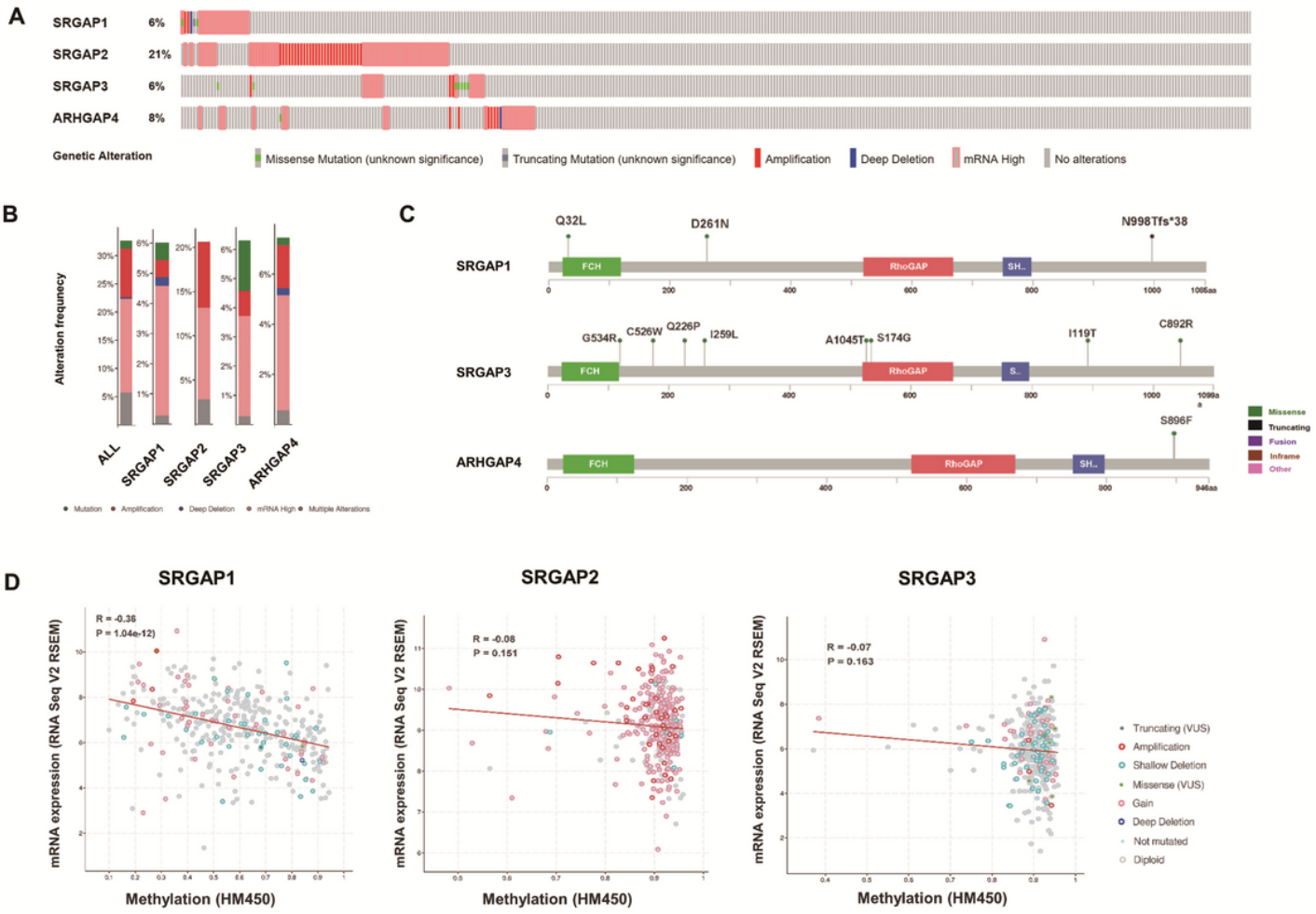

Figure 2

Genetic alterations of SRGAPs in HCC. (A) The OncoPrint visual summarized genetic variations of SRGAPs in TCGA dataset. (B) Alteration frequency details of SRGAPs in HCC. (C) Protein structure mutation details of SRGAP1, SRGAP2 and ARHGAP4 in HCC. (D) DNA methylation status of SRGAP1, SRGAP2 and SRGAP3 in HCC.

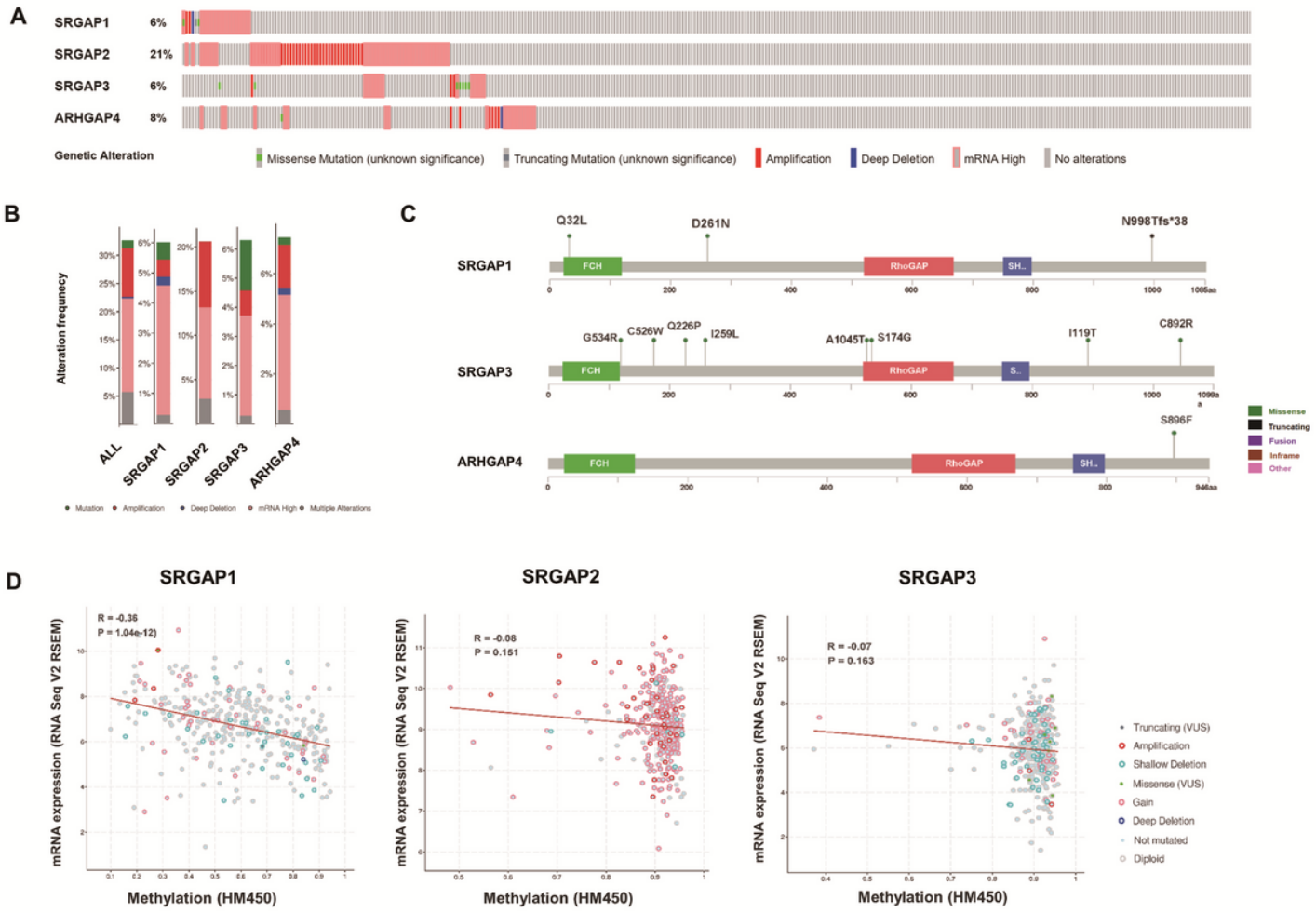

Figure 2

Genetic alterations of SRGAPs in HCC. (A) The OncoPrint visual summarized genetic variations of SRGAPs in TCGA dataset. (B) Alteration frequency details of SRGAPs in HCC. (C) Protein structure mutation details of SRGAP1, SRGAP2 and ARHGAP4 in HCC. (D) DNA methylation status of SRGAP1, SRGAP2 and SRGAP3 in HCC.

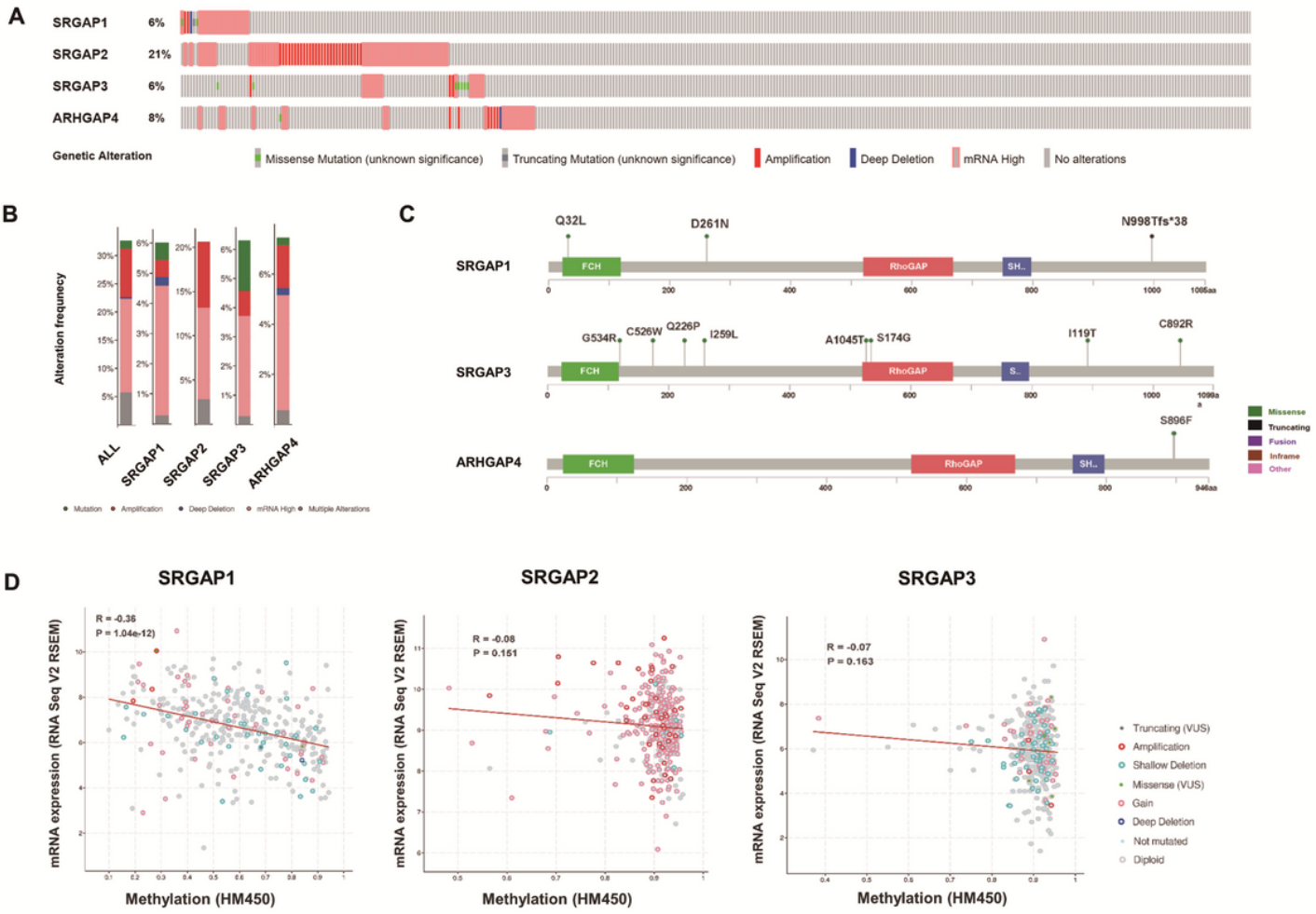

Figure 2

Genetic alterations of SRGAPs in HCC. (A) The OncoPrint visual summarized genetic variations of SRGAPs in TCGA dataset. (B) Alteration frequency details of SRGAPs in HCC. (C) Protein structure mutation details of SRGAP1, SRGAP2 and ARHGAP4 in HCC. (D) DNA methylation status of SRGAP1, SRGAP2 and SRGAP3 in HCC.

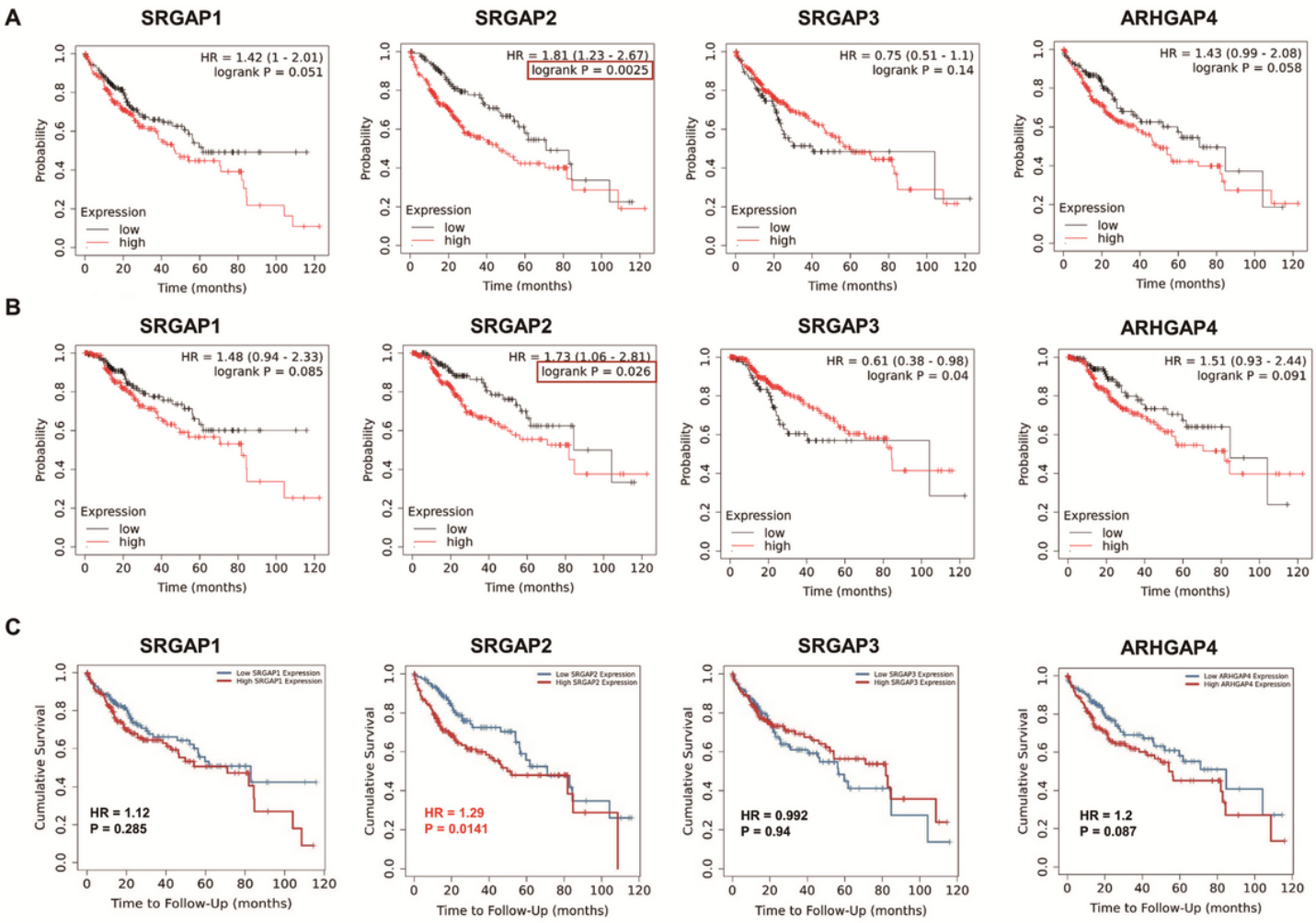

Figure 3

Prognostic values of SRGAPs in HCC. (A) Overall survival (OS) analysis of SRGAPs in HCC using Kaplan–Meier plotter (n=371). (B) Disease specific survival analysis (DSS) of SRGAPs in HCC using Kaplan–Meier plotter (n=371). (C) Multivariate Cox regression analysis of SRGAP2, age, gender, race, stage, purity in relation to OS of HCC patients in TCGA dataset (n=371). * P < 0.05, **P <0.01, *** P <0.001, **** P <0.0001.

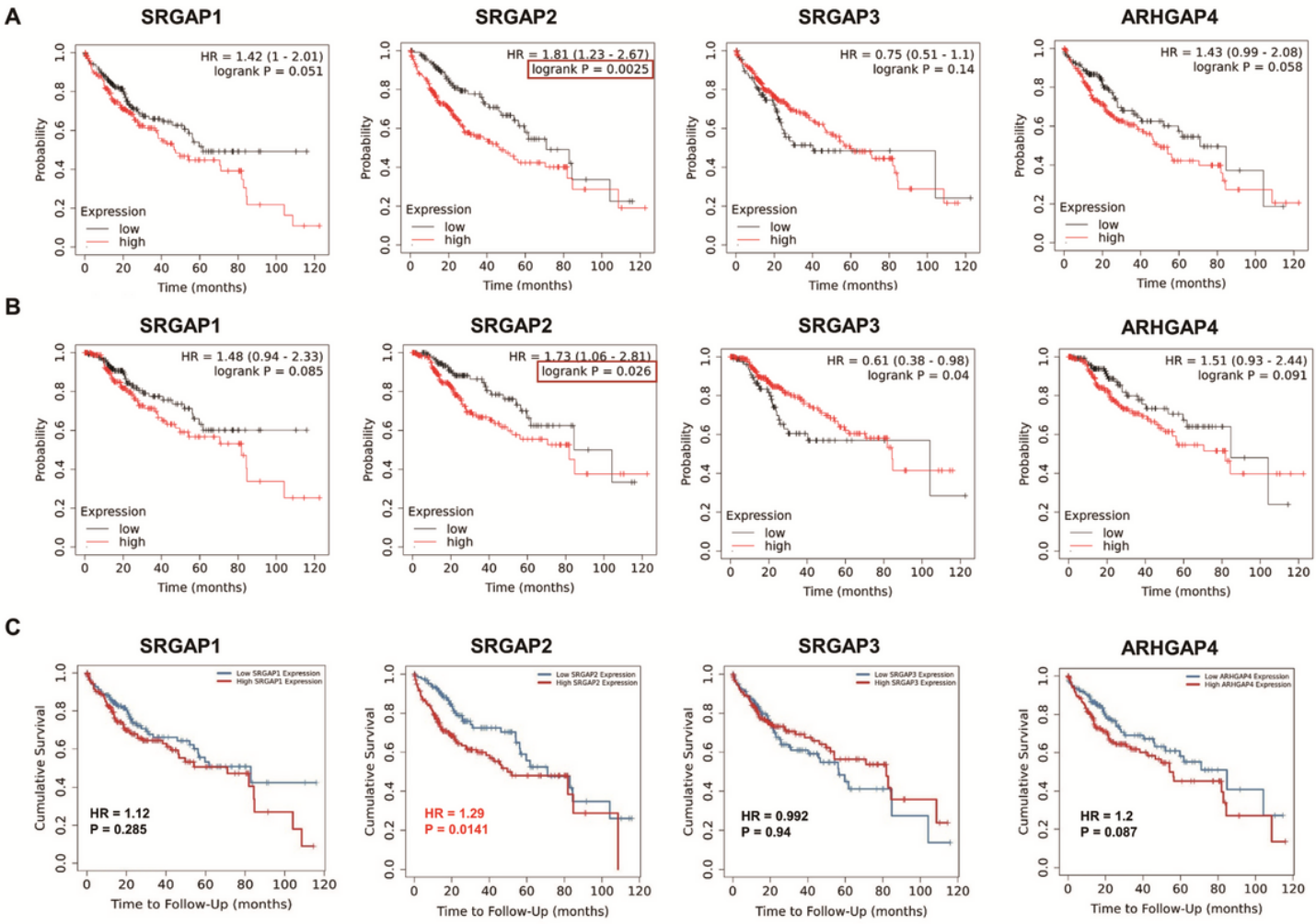

Figure 3

Prognostic values of SRGAPs in HCC. (A) Overall survival (OS) analysis of SRGAPs in HCC using Kaplan–Meier plotter (n=371). (B) Disease specific survival analysis (DSS) of SRGAPs in HCC using Kaplan–Meier plotter (n=371). (C) Multivariate Cox regression analysis of SRGAP2, age, gender, race, stage, purity in relation to OS of HCC patients in TCGA dataset (n=371). * P < 0.05, **P <0.01, *** P <0.001, **** P <0.0001.

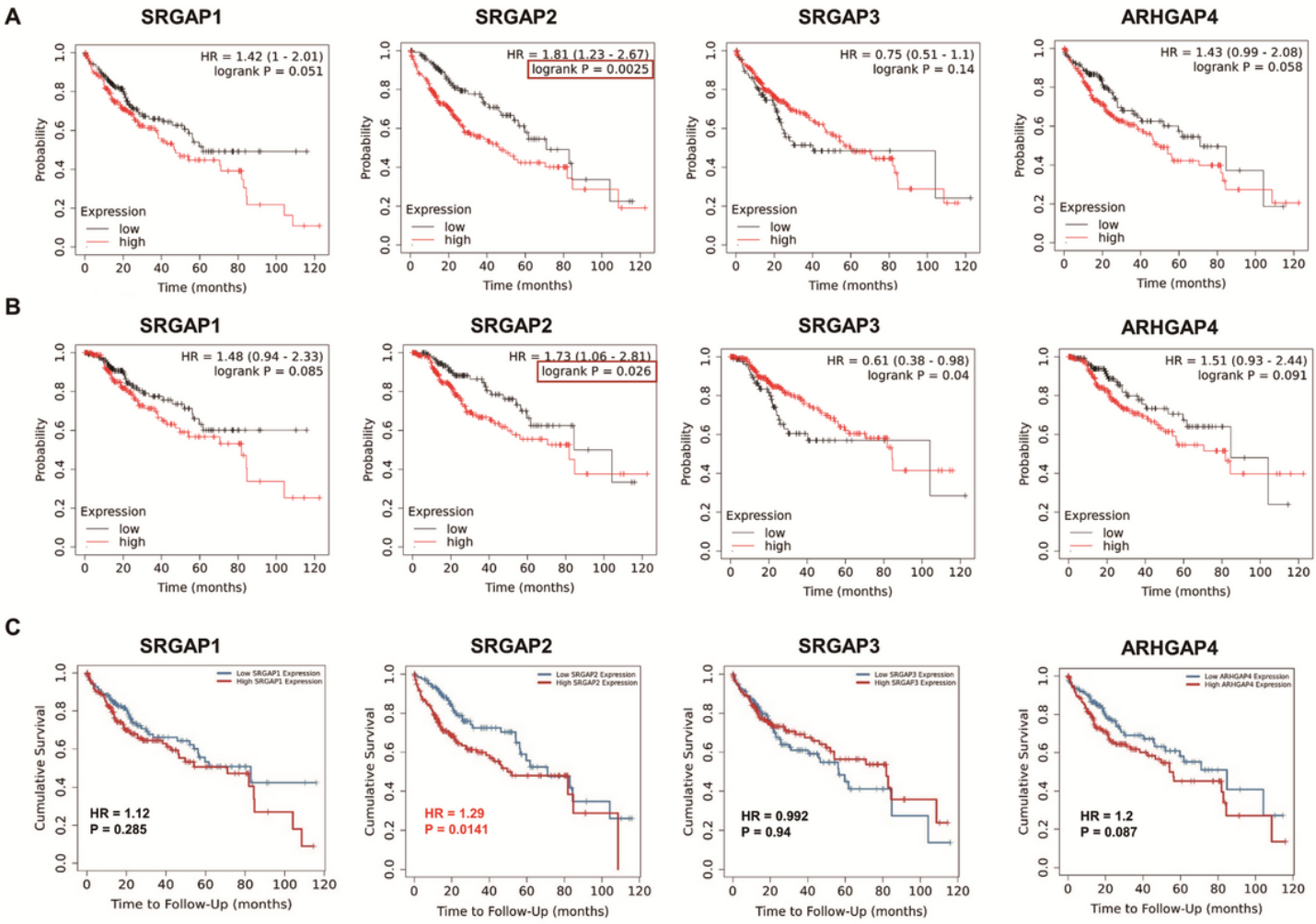

Figure 3

Prognostic values of SRGAPs in HCC. (A) Overall survival (OS) analysis of SRGAPs in HCC using Kaplan–Meier plotter (n=371). (B) Disease specific survival analysis (DSS) of SRGAPs in HCC using Kaplan–Meier plotter (n=371). (C) Multivariate Cox regression analysis of SRGAP2, age, gender, race, stage, purity in relation to OS of HCC patients in TCGA dataset (n=371). * P < 0.05, **P <0.01, *** P <0.001, **** P <0.0001.

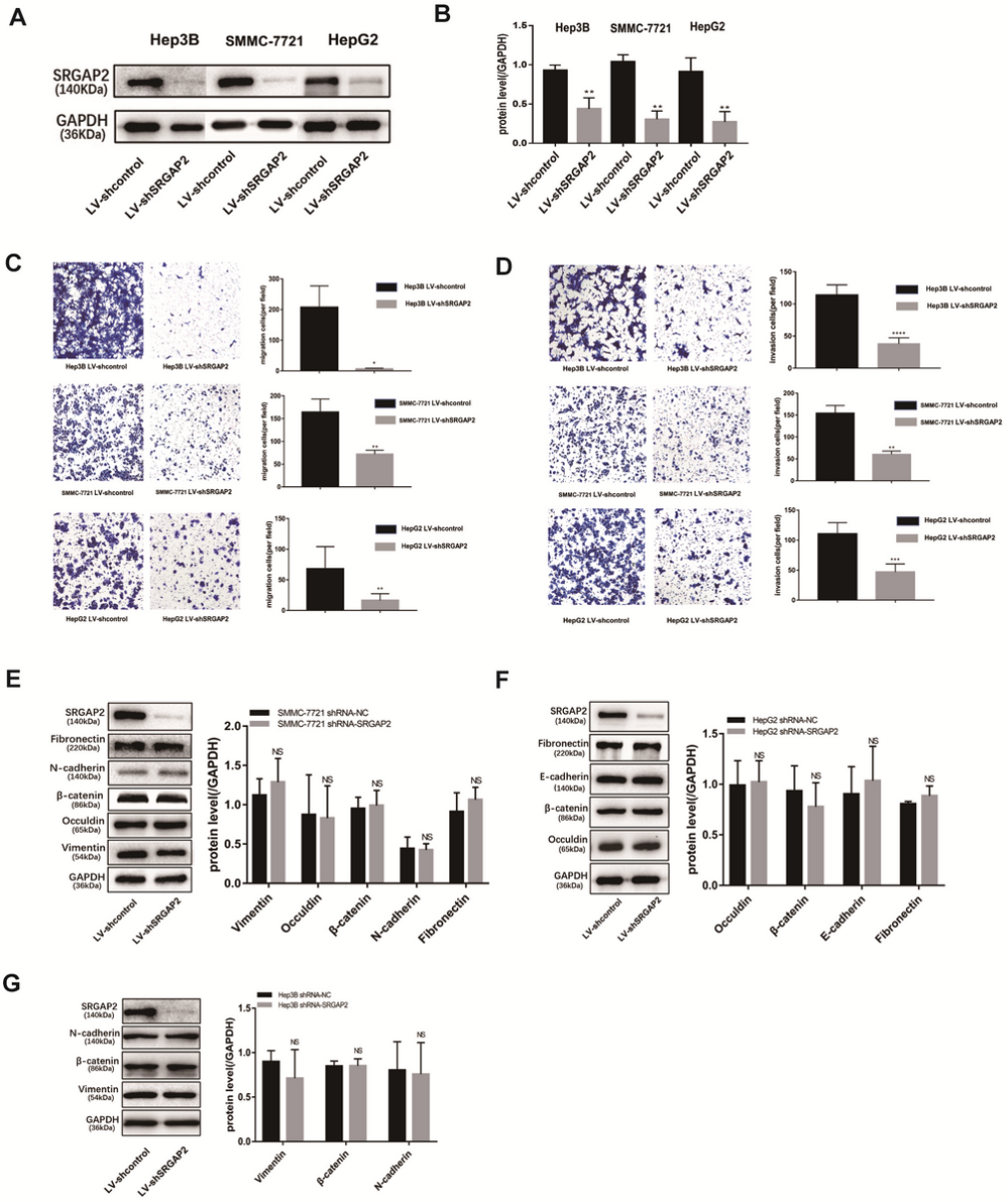

Figure 4

Silencing SRGAP2 inhibited the migration and invasion of HCC cells. (A) Western blot showed the protein expression levels of SRGAP2 in Hep3B, SMMC-7721 and HepG2 cells transfected with LV-shSRGAP2 and LV-shcontrol. (B) Relative protein levels (SRGAP2/GAPDH) in (A) were quantified by ImageJ. (C) Decreased SRGAP2 remarkably inhibited the migration ability of Hep3B, SMMC-7721 and HepG2 cells that was assessed by transwell assays. (D) Down-regulating SRGAP2 obviously inhibited the invasion capability of Hep3B, SMMC-7721 and HepG2 cells that was assessed by transwell assays. (E), (F) and (G) Representative images of Western blot showed the expression changes of epithelial and mesenchymal markers after SRGAP2 silencing in Hep3B (E), SMMC-7721(F) and HepG2 (G) cells, respectively.

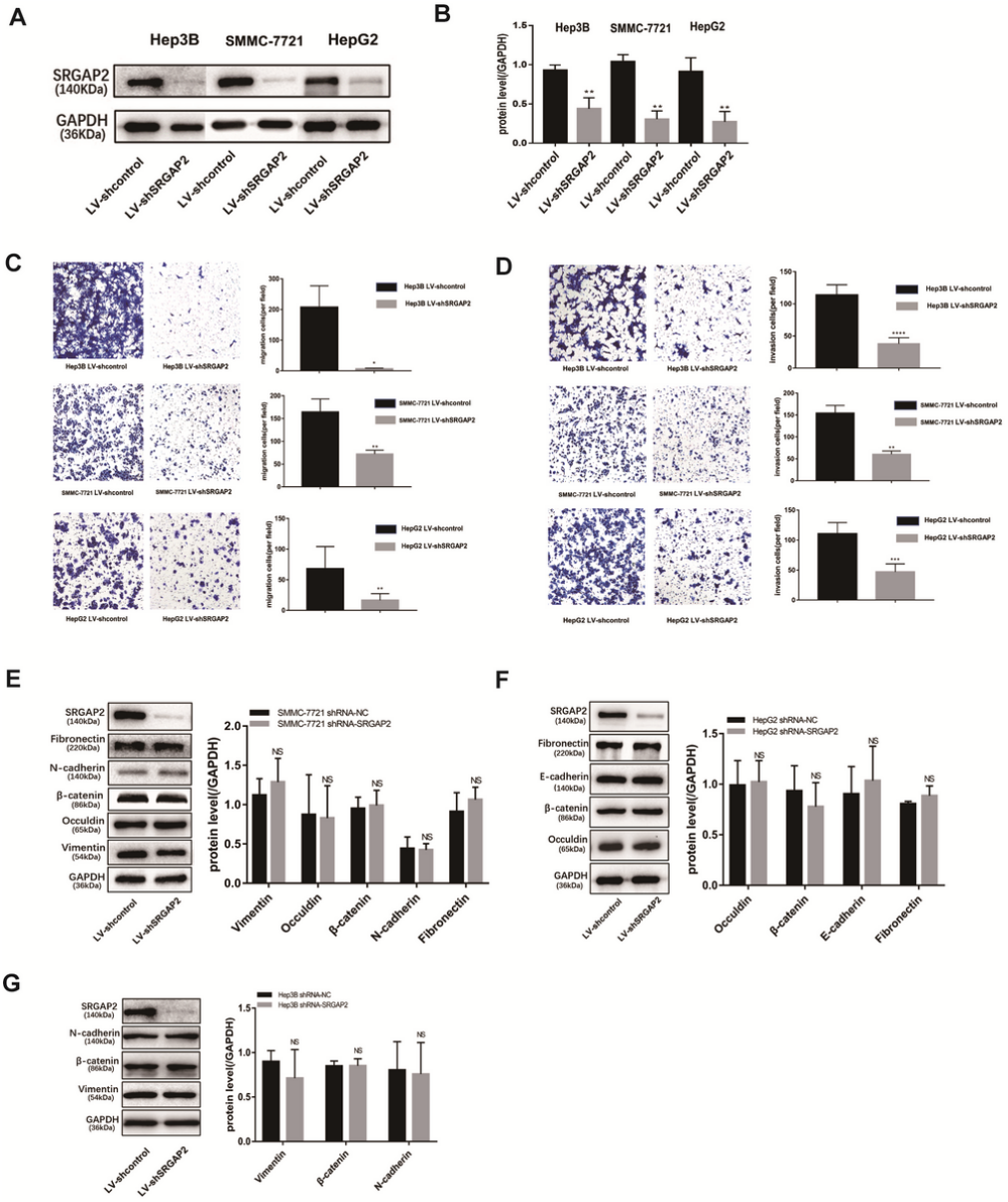

Figure 4

Silencing SRGAP2 inhibited the migration and invasion of HCC cells. (A) Western blot showed the protein expression levels of SRGAP2 in Hep3B, SMMC-7721 and HepG2 cells transfected with LV-shSRGAP2 and LV-shcontrol. (B) Relative protein levels (SRGAP2/GAPDH) in (A) were quantified by ImageJ. (C) Decreased SRGAP2 remarkably inhibited the migration ability of Hep3B, SMMC-7721 and HepG2 cells that was assessed by transwell assays. (D) Down-regulating SRGAP2 obviously inhibited the invasion capability of Hep3B, SMMC-7721 and HepG2 cells that was assessed by transwell assays. (E), (F) and (G) Representative images of Western blot showed the expression changes of epithelial and mesenchymal markers after SRGAP2 silencing in Hep3B (E), SMMC-7721(F) and HepG2 (G) cells, respectively.

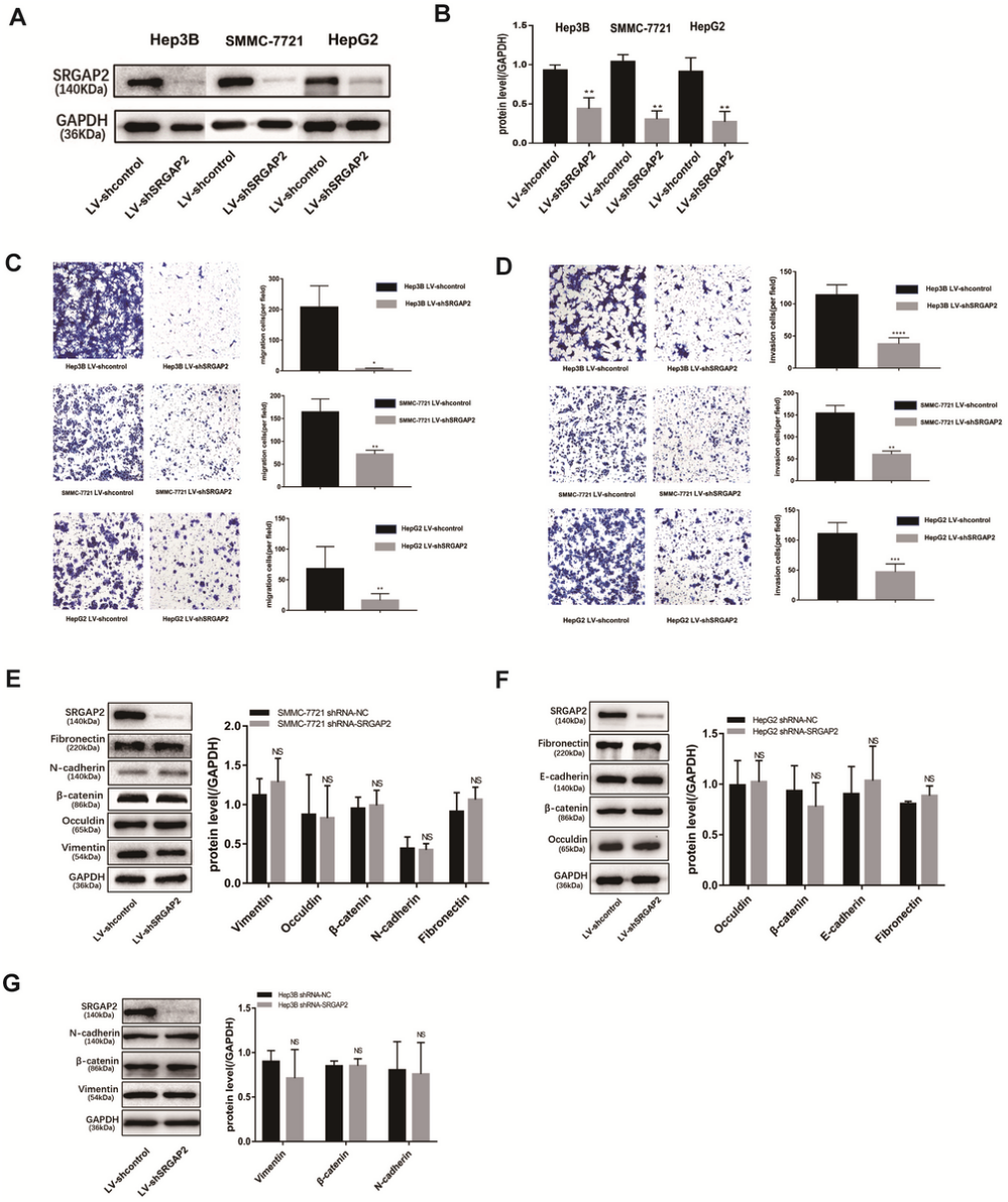

Figure 4

Silencing SRGAP2 inhibited the migration and invasion of HCC cells. (A) Western blot showed the protein expression levels of SRGAP2 in Hep3B, SMMC-7721 and HepG2 cells transfected with LV-shSRGAP2 and LV-shcontrol. (B) Relative protein levels (SRGAP2/GAPDH) in (A) were quantified by ImageJ. (C) Decreased SRGAP2 remarkably inhibited the migration ability of Hep3B, SMMC-7721 and HepG2 cells that was assessed by transwell assays. (D) Down-regulating SRGAP2 obviously inhibited the invasion capability of Hep3B, SMMC-7721 and HepG2 cells that was assessed by transwell assays. (E), (F) and (G) Representative images of Western blot showed the expression changes of epithelial and mesenchymal markers after SRGAP2 silencing in Hep3B (E), SMMC-7721(F) and HepG2 (G) cells, respectively.

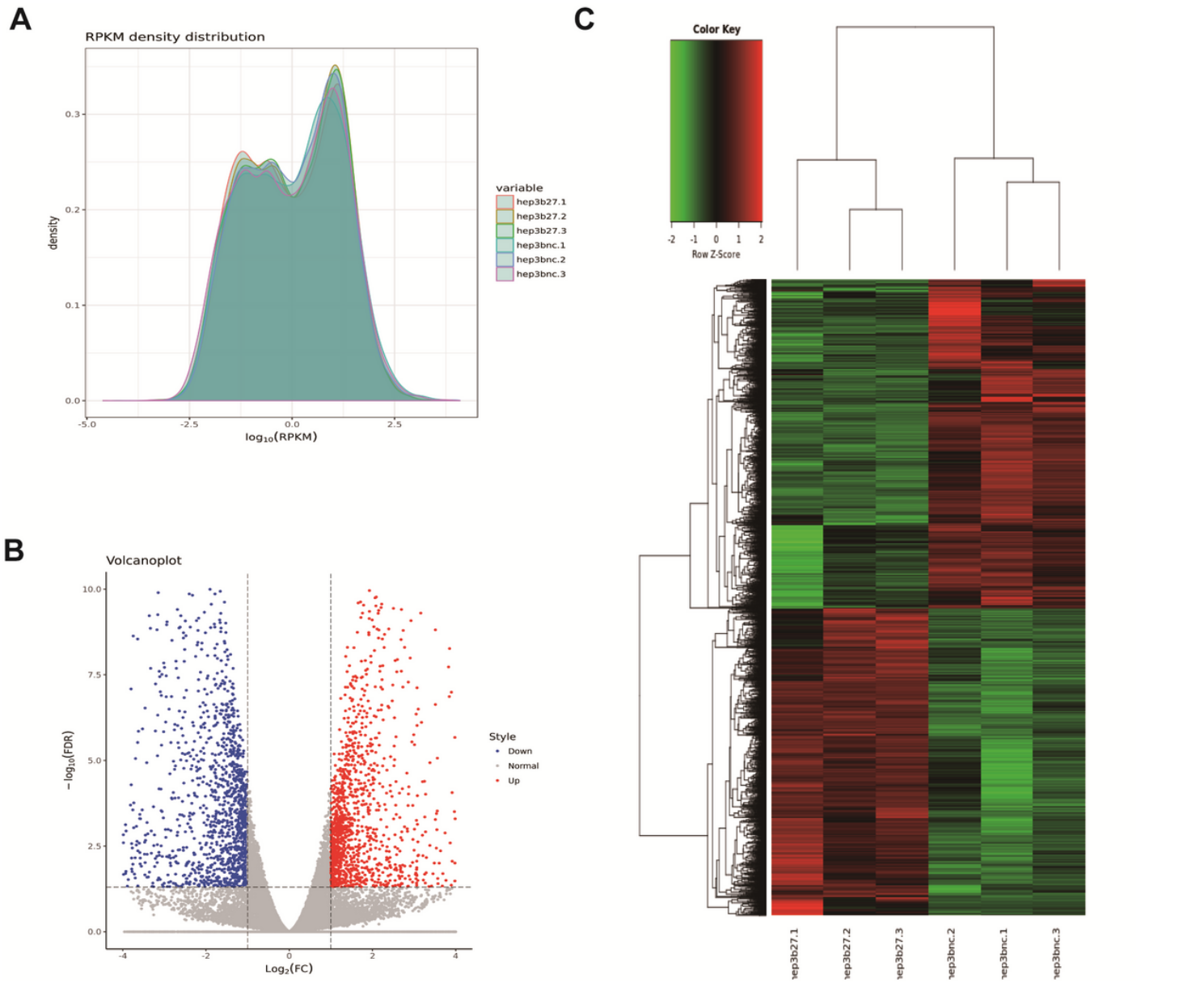

Figure 5

High-throughput RNA sequencing of HCC cells (Hep3B with LV-shSRGAP2 and LV-shcontrol). (A) Density analysis of these 6 samples. (B) Volcano map showed all differentially expressed genes from high-throughput RNA sequencing. (C) The heat map of upregulated and downregulated genes from high-throughput RNA sequencing.

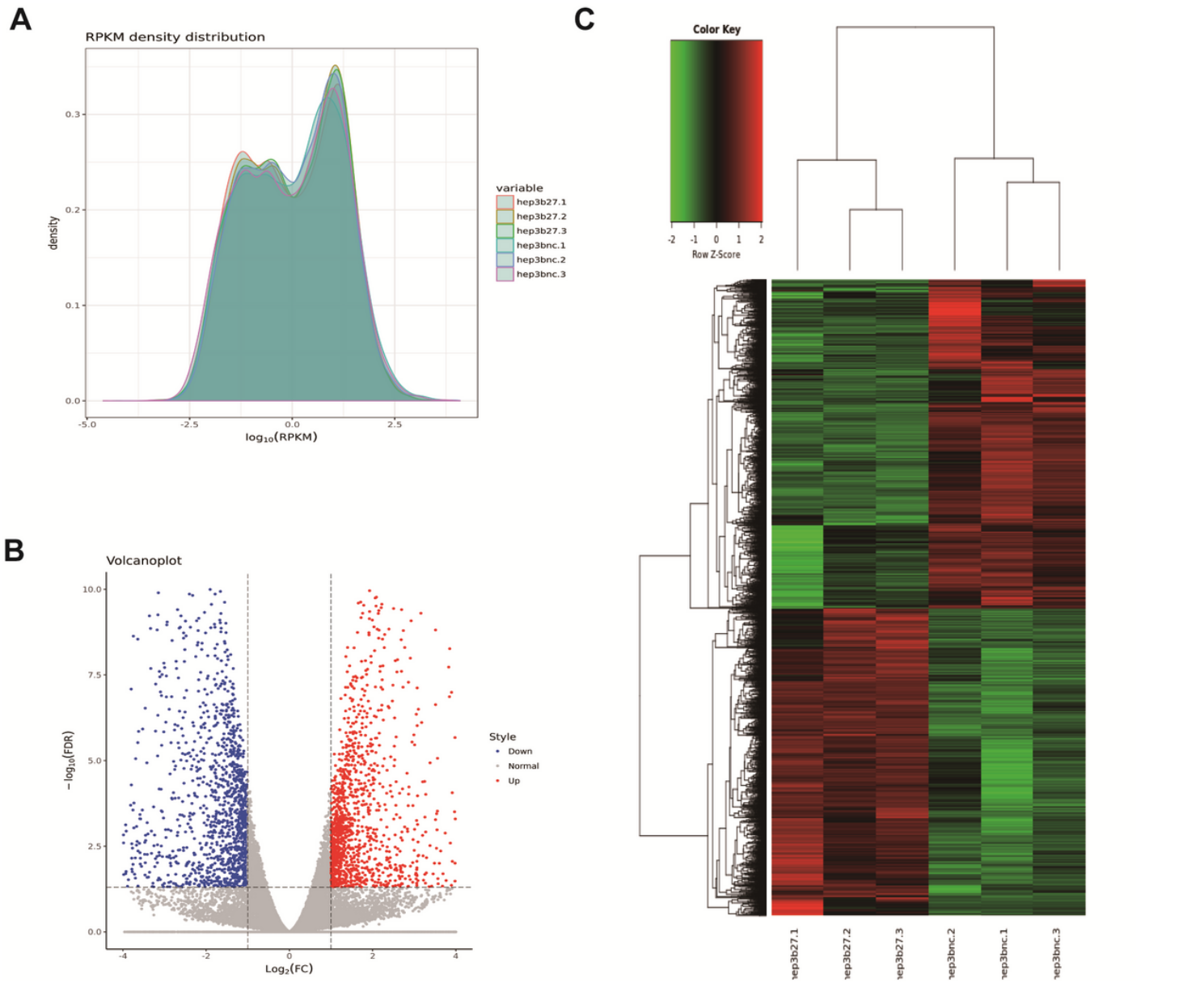

Figure 5

High-throughput RNA sequencing of HCC cells (Hep3B with LV-shSRGAP2 and LV-shcontrol). (A) Density analysis of these 6 samples. (B) Volcano map showed all differentially expressed genes from high-throughput RNA sequencing. (C) The heat map of upregulated and downregulated genes from high-throughput RNA sequencing.

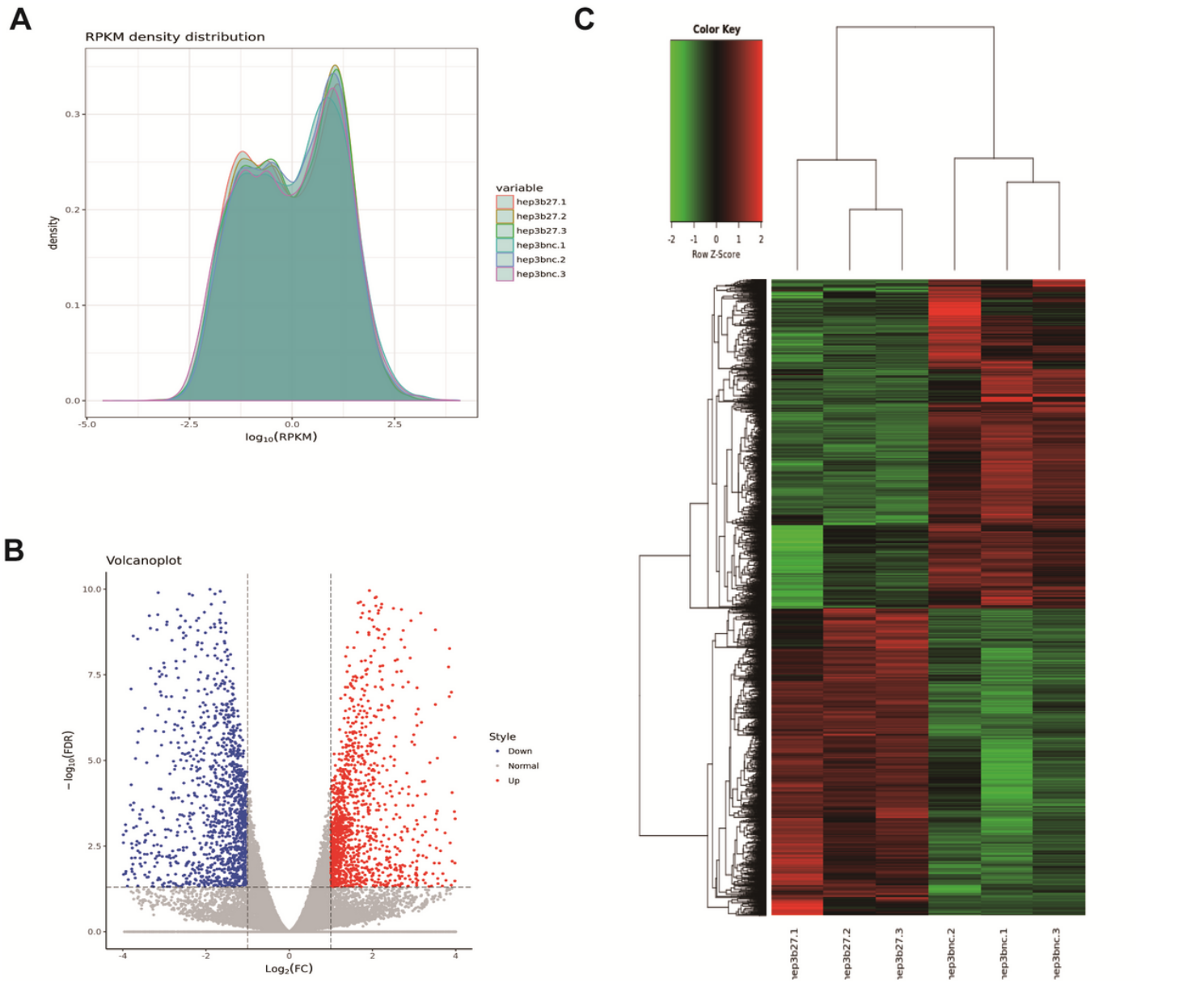

Figure 5

High-throughput RNA sequencing of HCC cells (Hep3B with LV-shSRGAP2 and LV-shcontrol). (A) Density analysis of these 6 samples. (B) Volcano map showed all differentially expressed genes from high-throughput RNA sequencing. (C) The heat map of upregulated and downregulated genes from high-throughput RNA sequencing.

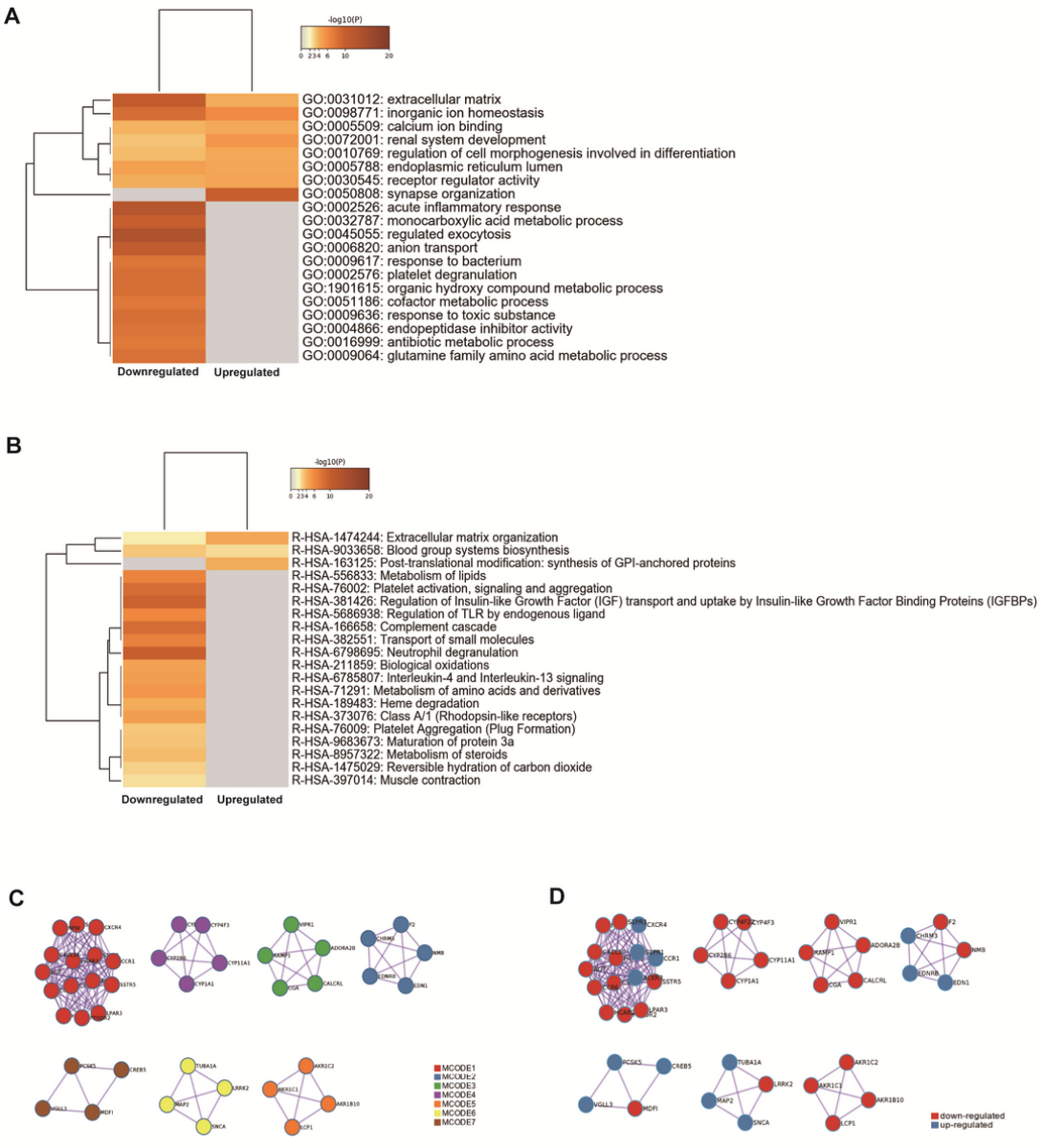

Figure 6

Functional enrichment analysis of SRGAP2-associated genes in HCC based on high-throughput RNA sequencing. We selected the term between upregulated and downregulated groups with the best p-value within each cluster as its representative term and displayed them in a dendrogram. The heatmap cells were colored by their p-values and the white cells indicated the lack of enrichment for that term in the corresponding gene list. (A) Top 20 GO enrichment terms were listed in the dendrogram. (B) Top 20 Reactome enrichment terms were listed in the dendrogram. (C) MCODE components were identified from the merged network. Each MCODE network was assigned an individual color. (D) MCODE components were identified from the merged network. Network nodes were displayed as pies. Red color code for pie sector represented the downregulated-genes and blue color code for pie sector represented the upregulated-genes.

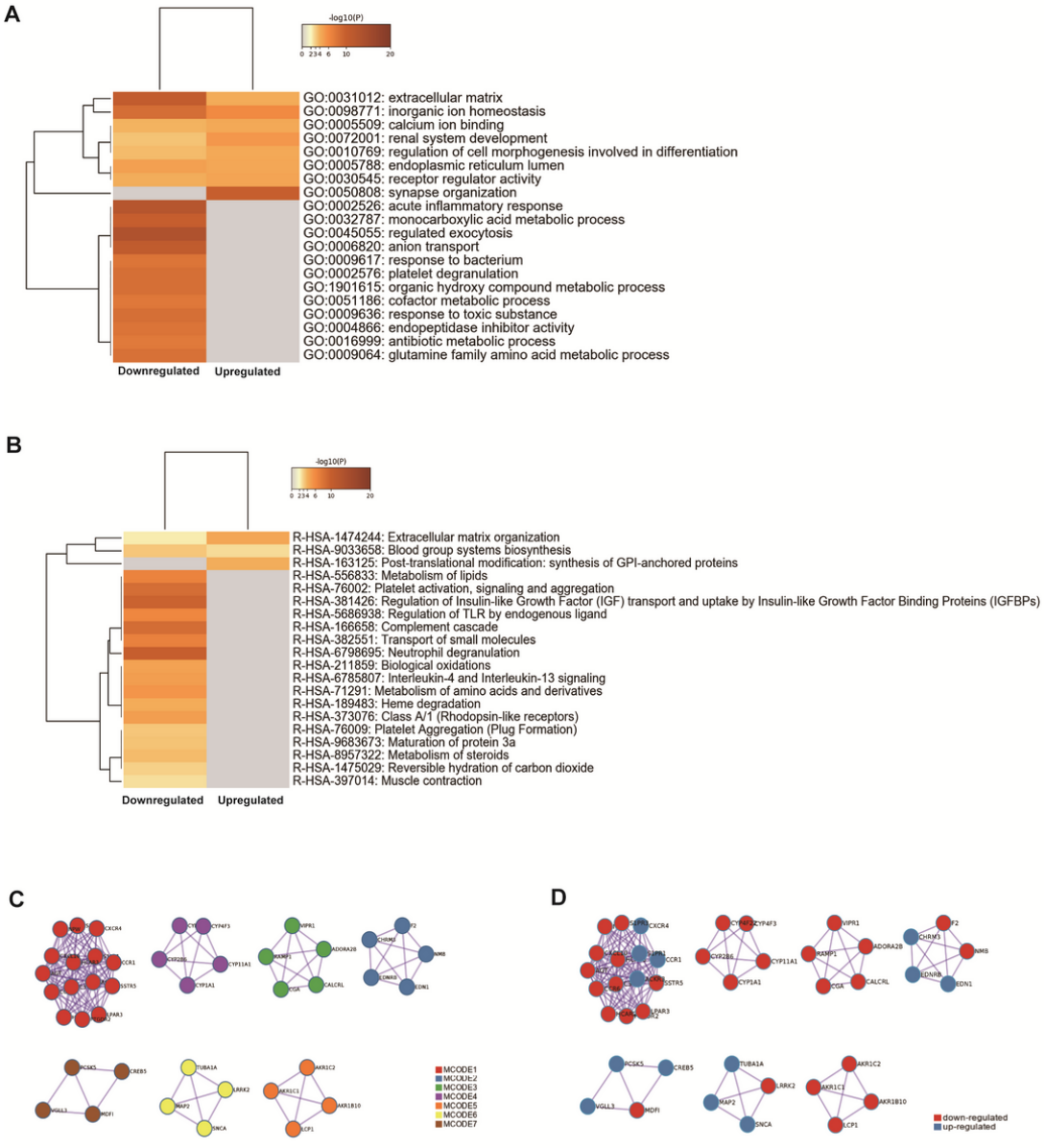

Figure 6

Functional enrichment analysis of SRGAP2-associated genes in HCC based on high-throughput RNA sequencing. We selected the term between upregulated and downregulated groups with the best p-value within each cluster as its representative term and displayed them in a dendrogram. The heatmap cells were colored by their p-values and the white cells indicated the lack of enrichment for that term in the corresponding gene list. (A) Top 20 GO enrichment terms were listed in the dendrogram. (B) Top 20 Reactome enrichment terms were listed in the dendrogram. (C) MCODE components were identified from the merged network. Each MCODE network was assigned an individual color. (D) MCODE components were identified from the merged network. Network nodes were displayed as pies. Red color code for pie sector represented the downregulated-genes and blue color code for pie sector represented the upregulated-genes.

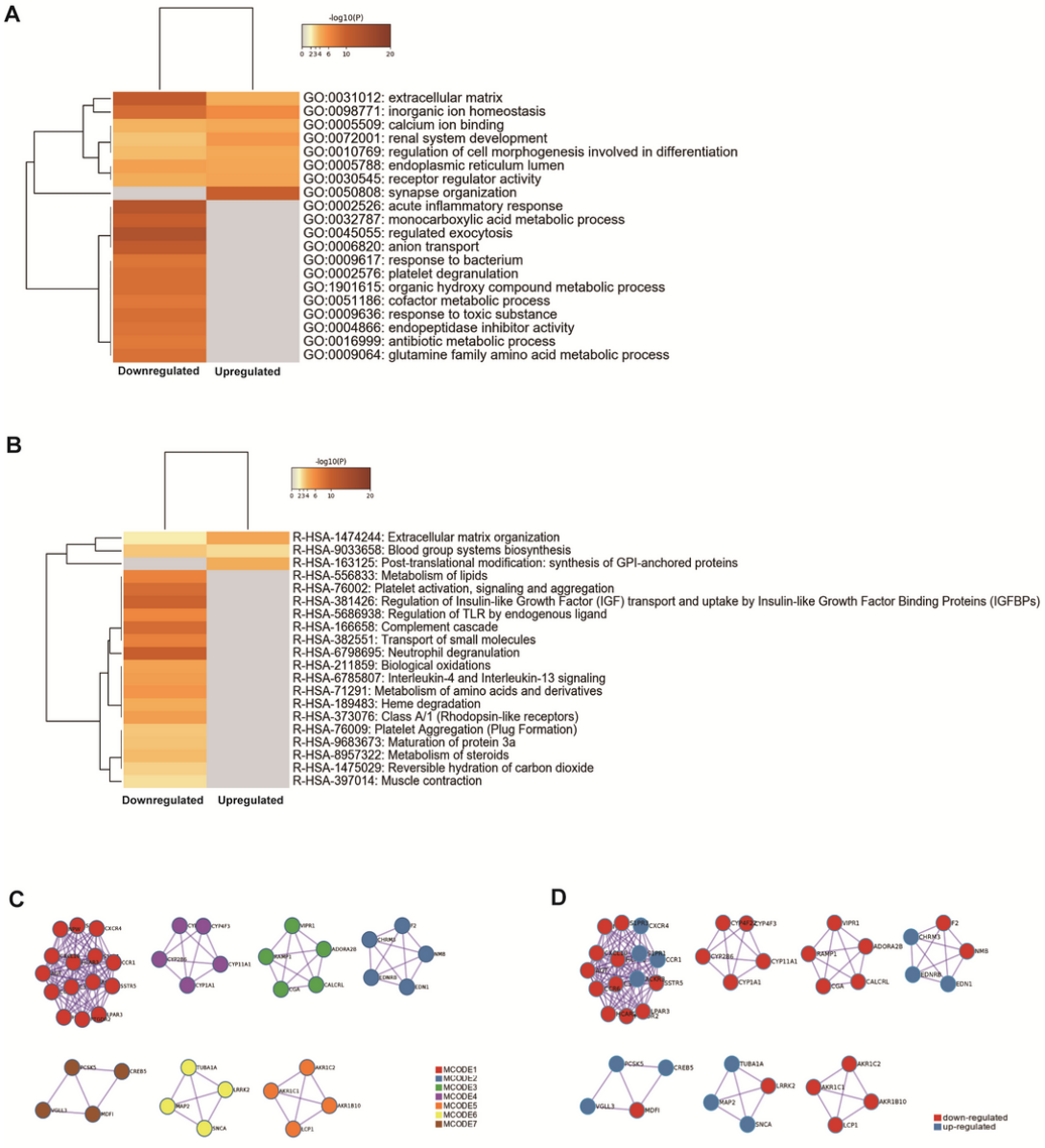

Figure 6

Functional enrichment analysis of SRGAP2-associated genes in HCC based on high-throughput RNA sequencing. We selected the term between upregulated and downregulated groups with the best p-value within each cluster as its representative term and displayed them in a dendrogram. The heatmap cells were colored by their p-values and the white cells indicated the lack of enrichment for that term in the corresponding gene list. (A) Top 20 GO enrichment terms were listed in the dendrogram. (B) Top 20 Reactome enrichment terms were listed in the dendrogram. (C) MCODE components were identified from the merged network. Each MCODE network was assigned an individual color. (D) MCODE components were identified from the merged network. Network nodes were displayed as pies. Red color code for pie sector represented the downregulated-genes and blue color code for pie sector represented the upregulated-genes.

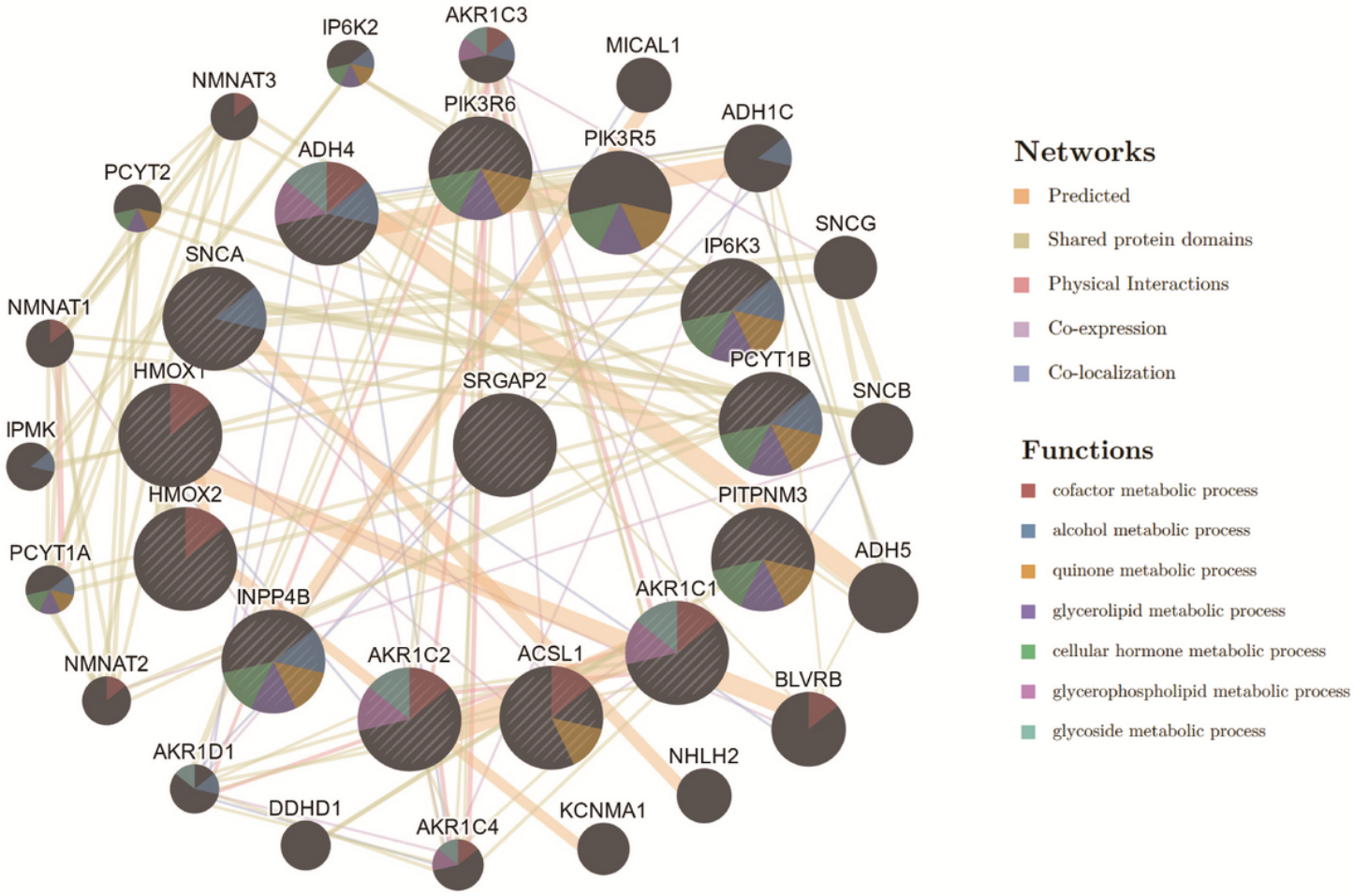

Figure 7

Gene-gene interaction network between SRGAP2 and the genes in metabolic signaling. Each node stood for an individual gene. The colors of inter-node connection lines stood for the types of gene-gene interactions. The color nodes indicated the underlying functions of respective genes.

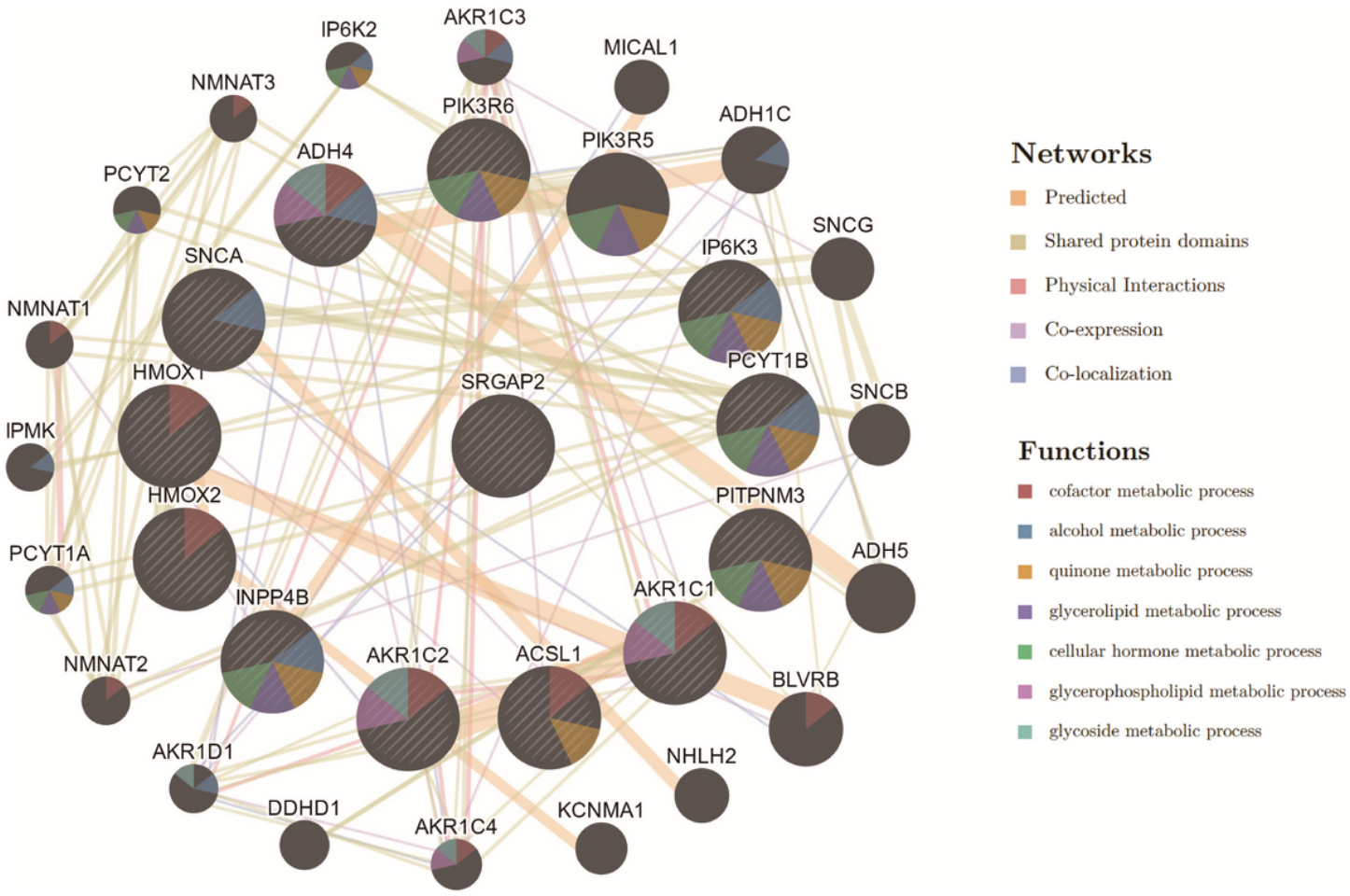

Figure 7

Gene-gene interaction network between SRGAP2 and the genes in metabolic signaling. Each node stood for an individual gene. The colors of inter-node connection lines stood for the types of gene-gene interactions. The color nodes indicated the underlying functions of respective genes.

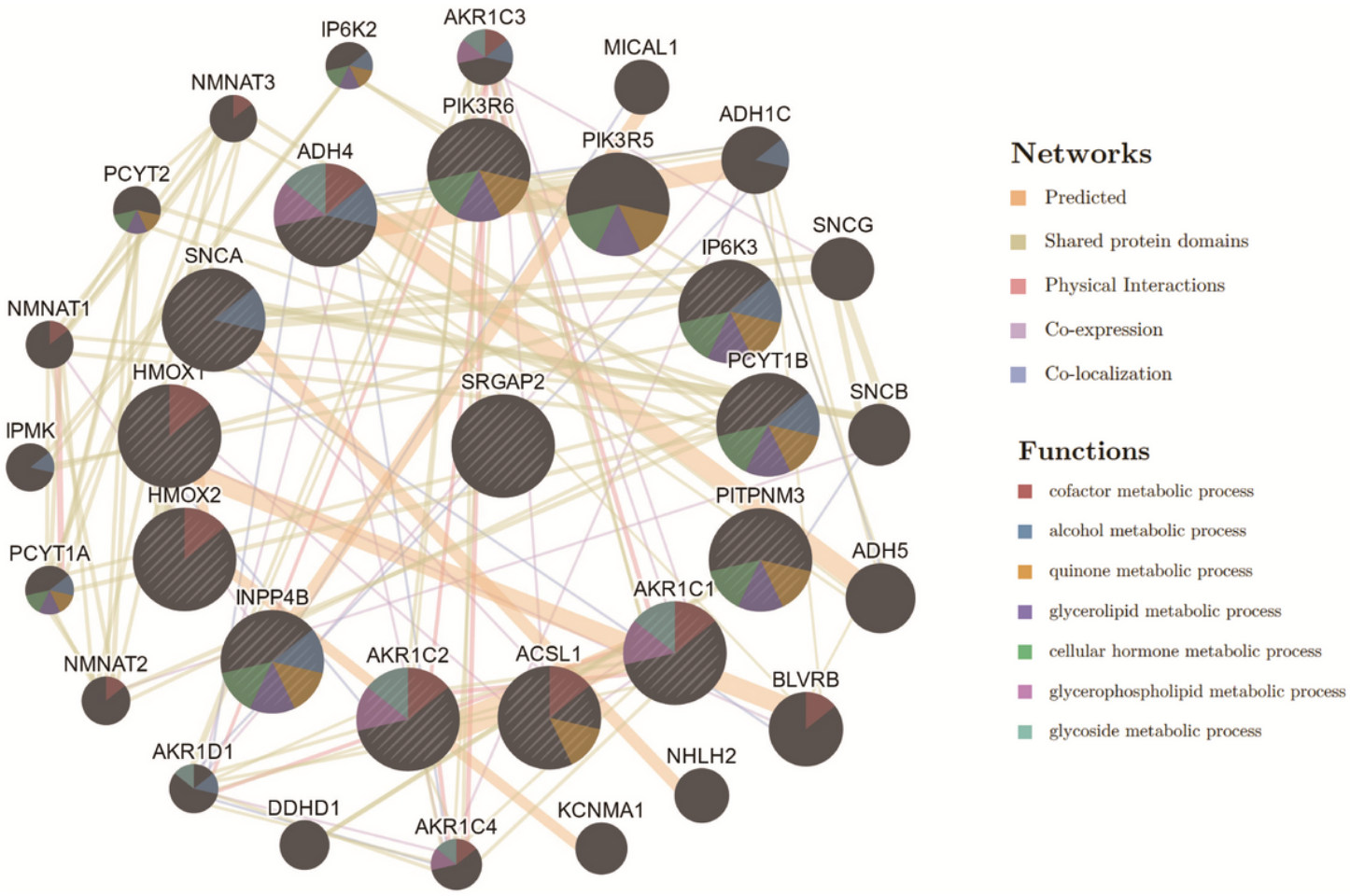

Figure 7

Gene-gene interaction network between SRGAP2 and the genes in metabolic signaling. Each node stood for an individual gene. The colors of inter-node connection lines stood for the types of gene-gene interactions. The color nodes indicated the underlying functions of respective genes.

Supplementary Files

This is a list of supplementary files associated with this preprint. Click to download.

- Supportinginformation.docx
- Supportinginformation.docx
- Supportinginformation.docx